MEASURING AND COMPUTING NATURAL GROUND-WATER RECHARGE

AT SITES IN SOUTH-CENTRAL KANSAS

By Marios A. Sophocleous and Charles A. Perry

U.S. GEOLOGICAL SURVEY

Water-Resources Investigations Report 87-4097

ii

CONTENTS

Page

Figure

Page

CONTENTS--Continued

CONTENTS--Continued

CONVERSION FACTORS

The following factors may be used to convert the metric (International System) units published herein to inch-pound units:

Multiply metric unit	By	To obtain inch-pound unit
millimeter (mm)	0.03937	inch (in.)
cubic centimeter (cm^3)	0.06102	cubic inch (in^3)
meter (m)	3.281	foot (ft)
cubic meter (m^3)	35.31	cubic foot (ft^3)
kilometer (km)	0.6214	mile (mi)
square kilometer (km^2)	0.3861	square mile (mi^2)
gram (gm)	0.002205	pound (lb)
degree Celsius (°C)	°F = 1.8 °C + 32	degree Fahrenheit (°F)
megapascal (MPa)	10	bar
megapascal (MPa)	10,000	millibar (mb)
calorie at 15 °C (cal)	3.087	foot-pound (ft-lb)
calorie at 15 °C (cal)	3.970×10^{-3}	British thermal unit (BTU)
langley per day [ly/d = (cal/cm^2)/d]	3.6879	British thermal unit per square foot per day [(BTU/ft^2)/d]
calories (at 15 °C) per gram (cal/gm)	1.8005	British thermal unit per pound (BTU/lb)
kilometer per hour (km/hr)	0.6214	mile per hour (mi/hr)
millimeter per day (mm/d)	0.03937	inch per day (in/d)
cubic meter per year (m^3/yr)	8.107×10^{-4}	acre-foot per year (acre-ft/yr)
gram per cubic centimeter (gm/cm^3)	62.43	pound per cubic foot (lb/ft^3)

Sea level: In this report "sea level" refers to the National Geodetic Vertical Datum of 1929 (NGVD of 1929)--a geodetic datum derived from a general adjustment of the first-order level nets of both the United States and Canada, formerly called "Mean Sea Level of 1929."

DEFINITION OF TERMS

Air entry pressure - The (negative) pressure of the pore water at which air begins to displace water, as evidenced by the first decrease in water content in the soil-water characteristic curve.

Available water capacity - Amount of water between field capacity and permanent wilting point that is available for plant use.

Capillary pressure (Moisture tension, matrix potential, negative pressure potential) - The equivalent negative pressure in the soil water resulting from capillary and adsorptive forces in the soil matrix. It is equal to the equivalent pressure that must be applied to the soil water to bring it to hydraulic equilibrium, through a porous permeable wall or membrane, with a pool of water of the same composition.

Hydraulic-conductivity function - A function or graph showing the hydraulic conductivity as a function of soil-water content or capillary pressure.

Hydraulic head - The altitude, with respect to a specified reference level, at which water stands in a piezometer open to a specific point in a geologic deposit. Its definition can be extended to strata above the water table if the piezometer is replaced by a tensiometer. The hydraulic head in systems under atmospheric pressure may be identified with a potential, expressed in terms of the height of a water column. More specifically, it can be identified with the sum of gravitational and capillary potentials and may be termed hydraulic potential. For unsaturated soil, the hydraulic heads referenced to the soil surface is equal to the soil suction or tension (-m) at a given point plus the depth (-m) to that point, with positive taken as upwards.

Hysteresis - Nonuniqueness in the relation between two quantities, in particular in the relation between the soil-water content and the soil-water capillary pressure.

Net radiation - The difference of the downward and upward solar and long-wave radiation flux passing through a horizontal plane just above the land surface.

Residual moisture - The minimum moisture content after the effects of gravity drainage and evapotranspiration become negligible.

Soil texture - The relative proportions of the various soil separates in a soil as described by the classes of soil texture shown in the following figure:

100 PERCENT CLAY (2 microns or less)

PERCENT CLAY

PERCENT SILT

CLAY

SILTY CLAY

SANDY CLAY

CLAY LOAM

SILTY CLAY LOAM

SANDY CLAY LOAM

LOAM

SILT LOAM

LOAMY SAND

SANDY LOAM

SILT

SAND

100 PERCENT SAND

100 PERCENT SILT

PERCENT SAND
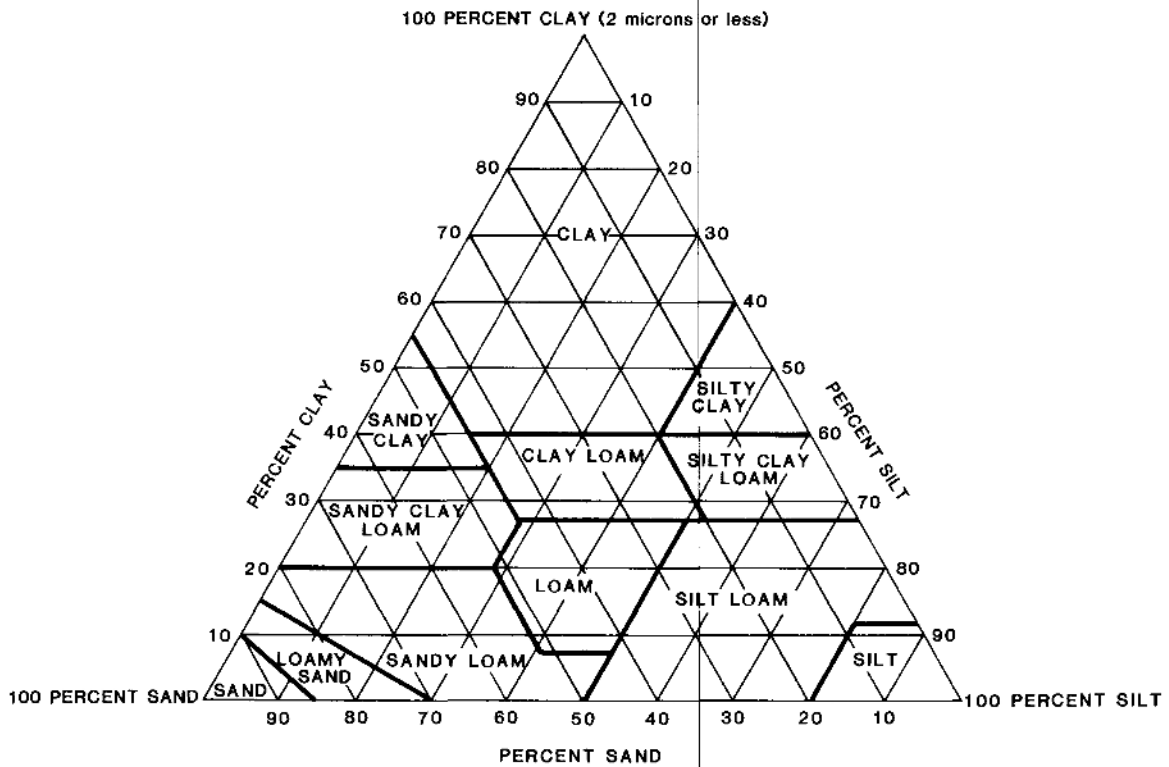
Soil-water characteristic (moisture-retention curve) - A graph showing the relation between soil-water content and moisture tension or capillary pressure.

Tensiometer - A device for measuring in situ the soil-water capillary pressure (or moisture tension or matrix potential) of water in soil; a porous, permeable ceramic cup connected through a water-filled tube to a manometer, vacuum gage, pressure transducer, or other pressure-measuring device.

Volumetric soil-water (or moisture) content - A ratio, usually expressed in percent, of the volume of water in the soil to the total bulk volume of the soil. It represents the depth ratio of soil water; that is, the depth of water per unit depth of soil.

Water-holding capacity - The moisture content when further reduction by gravity drainage is very slow.

Water saturation - The volume of water present in the soil relative to the volume of the pores. It is equal to the volumetric water content divided by the porosity.

MEASURING AND COMPUTING NATURAL GROUND-WATER RECHARGE

AT SITES IN SOUTH-CENTRAL KANSAS

By

Marios A. Sophocleous,

Kansas Geological Survey, Lawrence, Kansas

and

Charles A. Perry,

U.S. Geological Survey, Lawrence, Kansas

ABSTRACT

To measure the natural ground-water-recharge process, two sites in south-central Kansas were instrumented with sensors and data microloggers. The atmospheric-boundary layer and the unsaturated and saturated soil zones were monitored as a single regime. Data from the various sensors were collected using microloggers in combination with magnetic cassette tapes, graphical and digital recorders, and analog paper-tape recorders in order to automate data collection and processing. Direct observations also were used to evaluate the measurements.

Atmospheric sensors included an anemometer, a tipping-bucket rain gage, an air-temperature thermistor, a relative-humidity probe, a net radiometer, and a barometric-pressure transducer. Sensors in the unsaturated zone consisted of soil-temperature thermocouples, tensiometers coupled with pressure transducers and dial gages, gypsum blocks, and a neutron-moisture probe. The saturated-zone sensors consisted of a water-level pressure transducer, a conventional float gage connected to a variable potentiometer, soil thermocouples, and a number of multiple-depth piezometers.

Evaluation of the operation of these sensors and recorders indicates that certain types of equipment, such as pressure transducers, are very sensitive to environmental conditions. Extraordinary steps had to be taken to protect some of the equipment, whereas other equipment seemed to be reliable under all conditions. Based on such experiences, a number of suggestions aimed at improving instrumentation of recharge investigations are outlined.

The amounts and timing of ground-water recharge from precipitation over an approximately 19-month period were investigated at two instrumented sites in south-central Kansas. Precipitation and evapotranspiration data, taken together with soil-moisture profiles and storage changes, water fluxes in the unsaturated zone and hydraulic gradients in the saturated

1

zone at various depths, soil temperatures, water-table hydrographs, and water-level changes in nearby wells, describe the recharge process.

Antecedent moisture conditions and the thickness and nature of the unsaturated zone were found to be the major factors affecting recharge. Although the two instrumented sites are located in sand-dune environments in areas characterized by a shallow water table and a subhumid continental climate, a significant difference was observed in the estimated total recharge. The estimates ranged from less than 2.5 millimeters at the Zenith site, to approximately 154 millimeters at the Burrton site from February to June 1983. The principal reasons that the Burrton site had more recharge than the Zenith site were more precipitation, less evapotranspiration, and a shallower depth to the water table. Effective recharge took place only during late winter and spring. No summer or fall recharge was observed at either site during the observation period of this study.

INTRODUCTION

Ground-water-recharge rates of many regions in Kansas are less than present (1986) withdrawal rates or anticipated future demands, and the water resources presently are being mined in many areas (that is, permanent loss of aquifer storage is occurring). The Division of Water Resources of the Kansas State Board of Agriculture and local ground-water management districts use estimated recharge as an integral part of their renewable-water-supply management policies in order to administer ground-water rights. Improved estimates of recharge would make the renewable-water-supply calculations more accurate, and more effective management decisions would result. Ground-water recharge also is one of the most sensitive elements in digital ground-water flow models. Incorrect assumptions in representing recharge can invalidate the projections made by such models.

South-central Kansas is faced with appreciable ground-water-level declines and water-quality-degradation problems, in part as a result of large-scale agricultural development based on ground-water irrigation. At the same time, as a result of relatively large amounts of precipitation and generally sandy soils, south-central Kansas probably is experiencing appreciable amounts of ground-water recharge that need to be evaluated as part of effective ground-water management. The U.S. Geological Survey, in cooperation with the Kansas Geological Survey, conducted a study to evaluate natural recharge in south-central Kansas.

However, measurement of ground-water recharge is a major problem in many water-resource investigations. The conventional method of estimating recharge as precipitation minus evapotranspiration minus runoff, with allowance for changes in soil-moisture storage, is very sensitive to measurement errors and to the time scale of analysis; consequently, this commonly may lead to an underestimation of recharge (Howard and Lloyd, 1979). To avoid compounding errors in analysis of the hydrologic budget,

2

efforts need to be undertaken to obtain more direct estimates of vertical water fluxes at or near the water table. The approach presented in this report involves a detailed study of the combined unsaturated-saturated flow system. However, the problem of areal variability of recharge remains complex, and the previously mentioned, unsaturated-saturated approach may be impractical for regional applications, given the present state of technology, because of the large number of data-collection sites required and the cost of instrumentation.

Purpose and Scope

The purpose of the study described in this report was to measure natural ground-water recharge at two selected sites in south-central Kansas with potentially significant recharge environments. To achieve this goal, the following objectives were formulated:

(1) Evaluate and use state-of-the-art technology in onsite instrumentation and techniques to obtain reliable and frequent data related to ground-water recharge.

(2) Investigate the mechanisms of natural ground-water recharge by measuring the unsaturated-saturated flow regime as a unified system. Emphasis would be on precipitation-related recharge processes.

(3) Measure the amount and specify the timing of recharge for two sites in two major ground-water regions of Kansas--the Equus beds and Big Bend regions.

This report describes the experimental aspects of ground-water-recharge estimation. The approach followed in this study is similar to that followed by Freeze and Banner (1970), which was to measure the transport of moisture from the surface through the unsaturated zone, across the water table, and into the saturated ground-water flow system. Such a profile of ground-water recharge would consist of measuring the following hydrologic characteristics:

(a) Precipitation,
(b) Potential or actual evapotranspiration,
(c) Soil-water content at various depths,
(d) Change in soil-moisture storage in the unsaturated soil profile,
(e) Water fluxes at the deepest tensiometer-nest level above the water table and at or in the immediate vicinity of the water table,
(f) Soil-temperature anomalies that result from recharging-water influxes,
(g) Water-table altitudes,
(h) Saturated water fluxes or hydraulic gradients near the water table and deeper in the ground-water flow system, and
(i) Water-level changes in the general area of the recharge sites.

Background information for recharge profiles would include soil-texture profiles, soil-water characteristic curves (that is, the relation between

3

capillary pressure and soil-water content), and hydraulic-conductivity functions.

In this study, ground-water recharge was defined initially as that water which percolates into the lower limits of the unsaturated zone, reaches the water table, and causes measurable water-table rise. This definition was extended later to include amounts of recharge required for maintaining water-table rises already achieved from an immediately preceding effective recharge event.

Location and General Physical Setting of Recharge Sites

Two experimental sites were instrumented for this study. One site is located in the Equus beds area (Lohman and Frye, 1940) in Harvey County (Burrton site), northwest of the city of Wichita, while the other is in the Big Bend region in Reno County (Zenith site), west of Wichita (fig. 1). Principal aquifers referred to as the Big Bend aquifer and Equus beds aquifer in both areas are considered part of the regional High Plains aquifer and are used extensively for agricultural irrigation (fig. 1). The Equus beds aquifer also is used to satisfy a significant part of the

EXPLANATION
▲ BURRTON RECHARGE SITE
■ ZENITH RECHARGE SITE
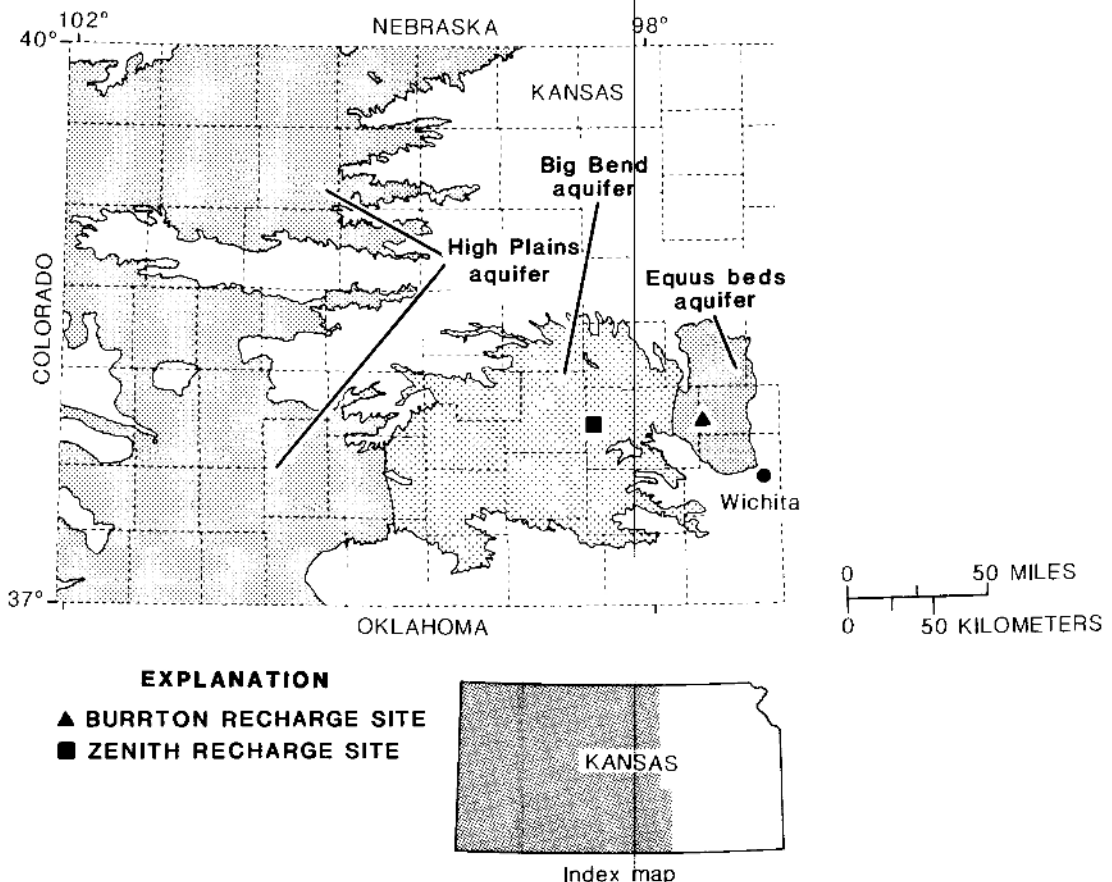
Figure 1.--Location of study area.

4

water needs of the city of Wichita. Both the Burrton and Zenith recharge sites are located in relatively flat, sand-dune environments. No well-established drainage patterns exist, indicating that surface runoff may be negligible. Rainfall either infiltrates directly into the sandy soil or accumulates in shallow depressions. The sites are covered by native mixed-grass vegetation.

Acknowledgments

GENERAL HYDROGEOLOGY OF THE RECHARGE SITES

Hydrometeorological Setting

The climate at the study sites is characterized by moderate precipitation, a wide range of temperatures, and moderately high average wind velocity. Ranges of precipitation, temperature, and evaporation throughout the year are shown in figure 2. Average annual precipitation is approximately 738 mm. The amount of precipitation, however, varies greatly from year to year and generally increases eastward across the State. The lowest average monthly precipitation is 18 mm during January, and the highest average is 113 mm during May. Approximately 72 percent of the annual precipitation falls from April to September (Rockers and others, 1966). Snowfall varies from year to year, but the average annual amount is approximately 508 mm.

Mean monthly temperature minima and maxima vary from -6.7 and 5.6 °C during January to 19.4 and 33.3 °C, respectively, during July. The mean annual temperature is 13.4 °C. The prevailing winds are southerly, averaging from 24 km/hr during March and April to 19 km/hr during July and August (Rockers and others, 1966). Because of the abundance of warm temperatures and relatively high wind speeds, pan evaporation at the city of Wichita averages 1,630 mm/yr (Farnsworth and Thompson, 1982). Average evaporation exceeds average precipitation for every month of the year. However, short-term (days to weeks) precipitation may exceed corresponding evaporation, resulting in ground-water recharge.

Surficial Geology and Soil Properties

A generalized surficial geology map of the study area is shown in figure 3. The recharge sites consist of unconsolidated deposits of predominantly Holocene and Pleistocene age overlying Permian bedrock. The unconsolidated deposits are of fluvial origin with sand beds generally lying between lenses of silt, clay, and sandy clay as can be inferred
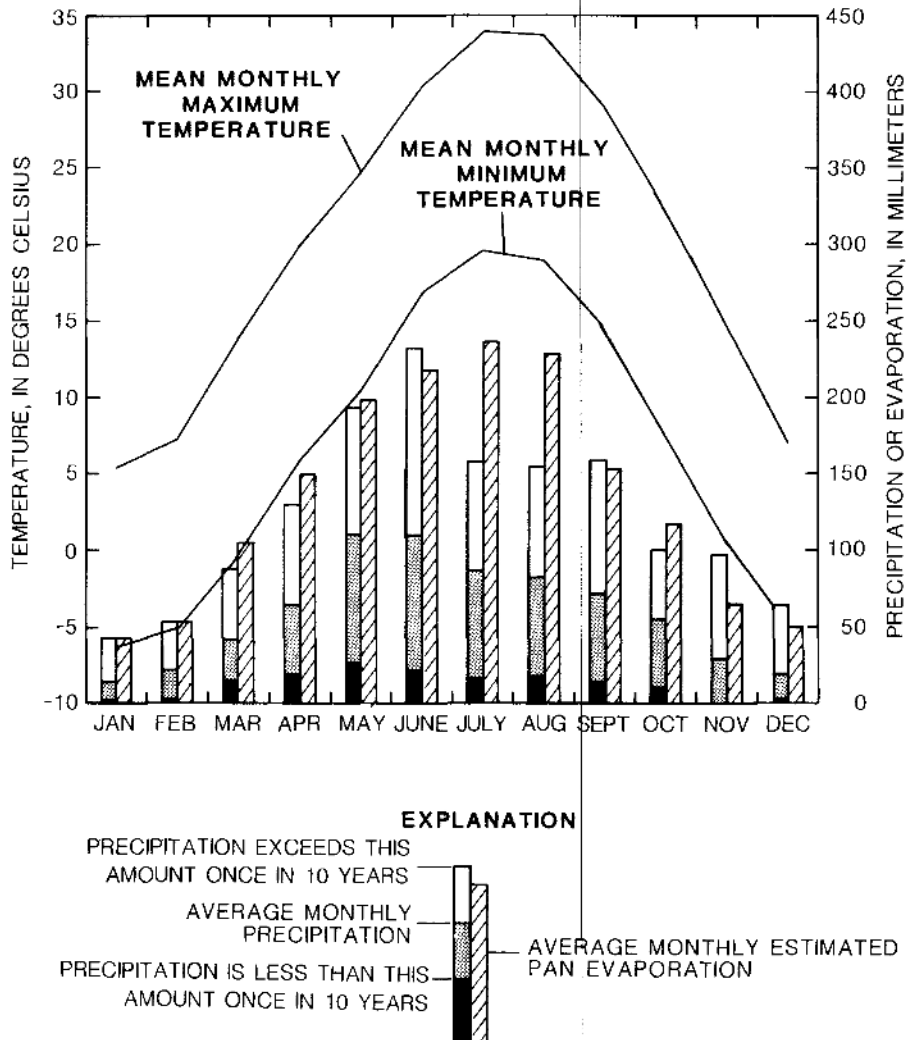
Figure 2.--Average monthly precipitation and temperature minima and maxima for Hutchinson and average monthly estimated "pan evaporation" for Wichita (data from Rockers and others, 1966; Farnsworth and Thompson, 1982).

from the natural gamma-ray logs at each of the recharge sites (fig. 4). Significant clay layers can be recognized at the 19- to 21-m and 23- to 25-m depth intervals for the Burrton site and at the 25- to 33-m depth interval for the Zenith site (fig. 4). For the most part, the fluvial deposits are covered by eolian deposits. A large sand-dune deposit, mostly underlain by discontinuous clay lenses, occurs in the area of the recharge sites (fig. 3).

The soil at the sites belongs to the Pratt series, which consists of deep, well-drained, gently undulating light-colored, fine sandy loam soils. These soils were formed in sandy eolian deposits and exhibit small available water capacities (Rockers and others, 1966).

The depth variation of soil-particle size, the corresponding soil texture, and the vertical saturated hydraulic conductivity for the Burrton
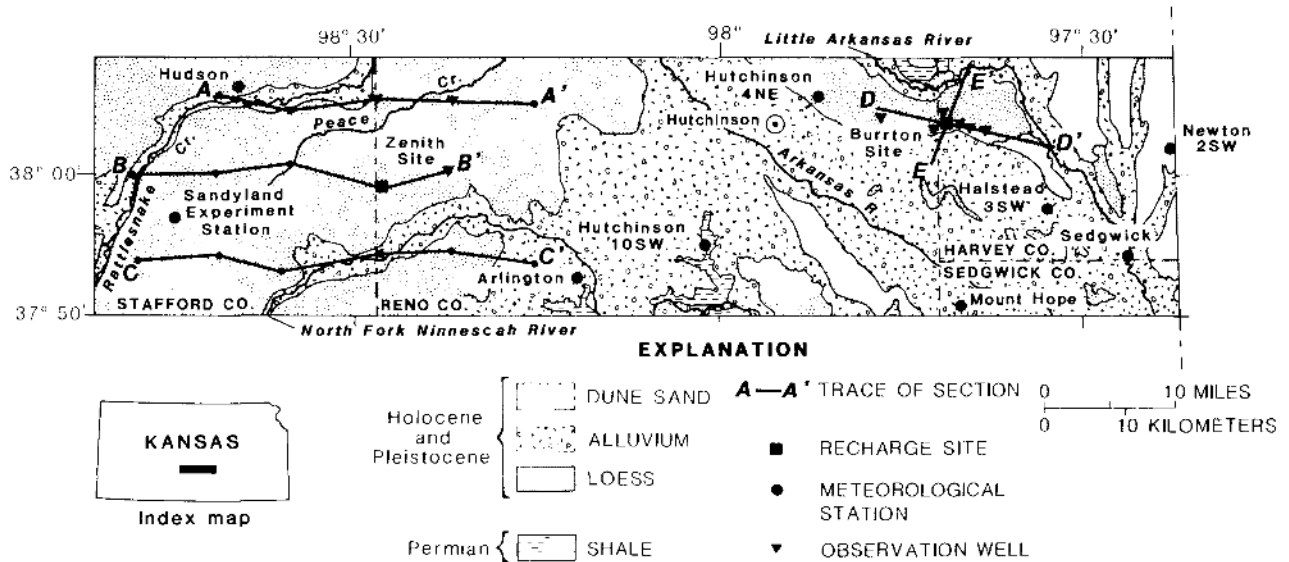
Figure 3.--Generalized surficial geology of study area (adapted from Kansas Geological Survey, 1964).

site are shown in figure 5 and for the Zenith site in figure 6. The water table at the Burrton site is much shallower and more variable with time than at the Zenith site, with the depth to water averaging approximately 1.2 to 1.5 m. The Zenith site is situated in soil that is similar to the Burrton site. The depth to the water table is approximately 5.2 m. This difference in depth to water table between the two sites is of major significance in the estimated amounts of recharge at each site, as will be shown. The saturated hydraulic conductivity of the soil above the water table generally decreases with depth at both sites. This conductivity pattern probably is due to the decreasing sand content and increasing bulk density of the soil with depth.

Shallow Ground-Water Flow System

Approximate directions of ground-water flow along the trace of sections shown in figure 3 are depicted in figures 7 and 8. These cross sections were drawn parallel to the general direction of flow so as to depict true gradients. The hydraulic-head data for the Burrton area shown in figure 7 were measured during 1978-81. A complete set of measurements for any single time was not available. The hydraulic-head data for the Zenith area (fig. 8) were determined from water levels measured in piezometer nests and wells during March 1982. Based on these data, equipotential lines were drawn, and principal directions of ground-water flow were indicated. From these and other more localized cross-sectional flow nets, both the Burrton and Zenith sites were identified as being ground-water-recharge sites (with ground water moving downwards away from the water table). A regional water-level gradient to the east exists in the general study area, as can be inferred also from figures 7 and 8 (see also Sophocleous, 1983).
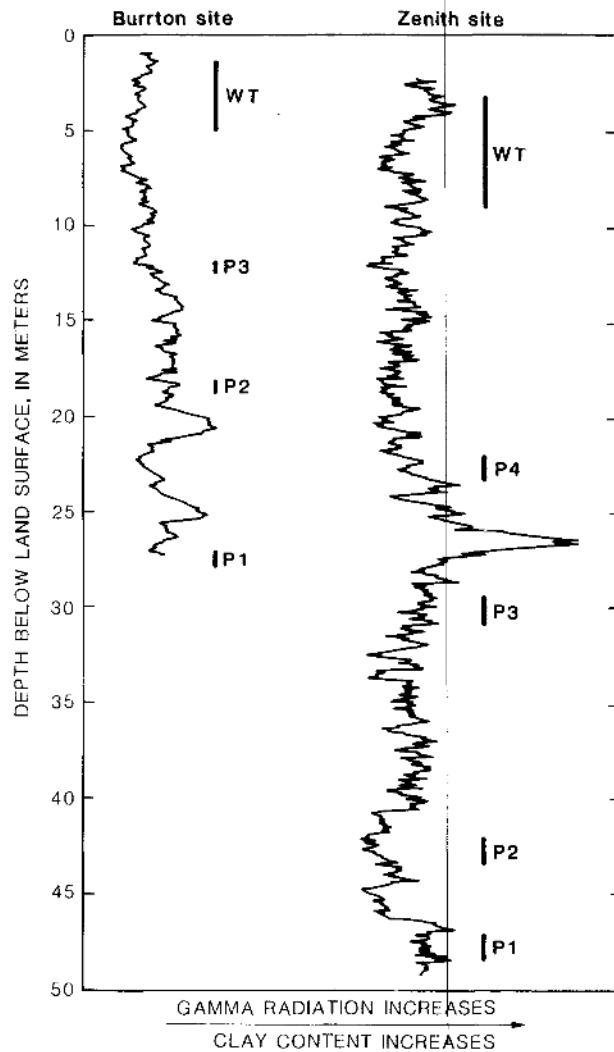
7

Figure 4.—Natural gamma-ray logs and piezometer-screen intervals for Burrton and Zenith sites.
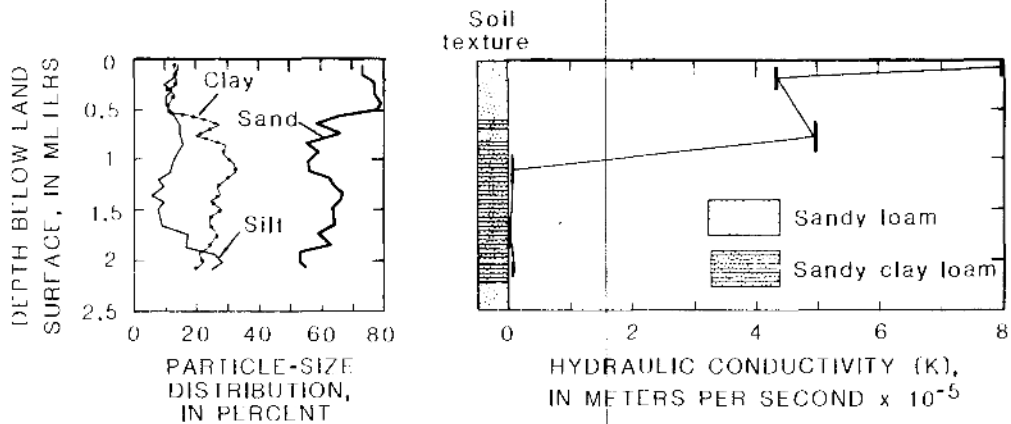
Figure 5.—Depth variation of soil-particle size, soil texture, and saturated hydraulic conductivity for Burrton site. (The vertical bars indicate that the soil sample was taken from indicated depth interval.)

8
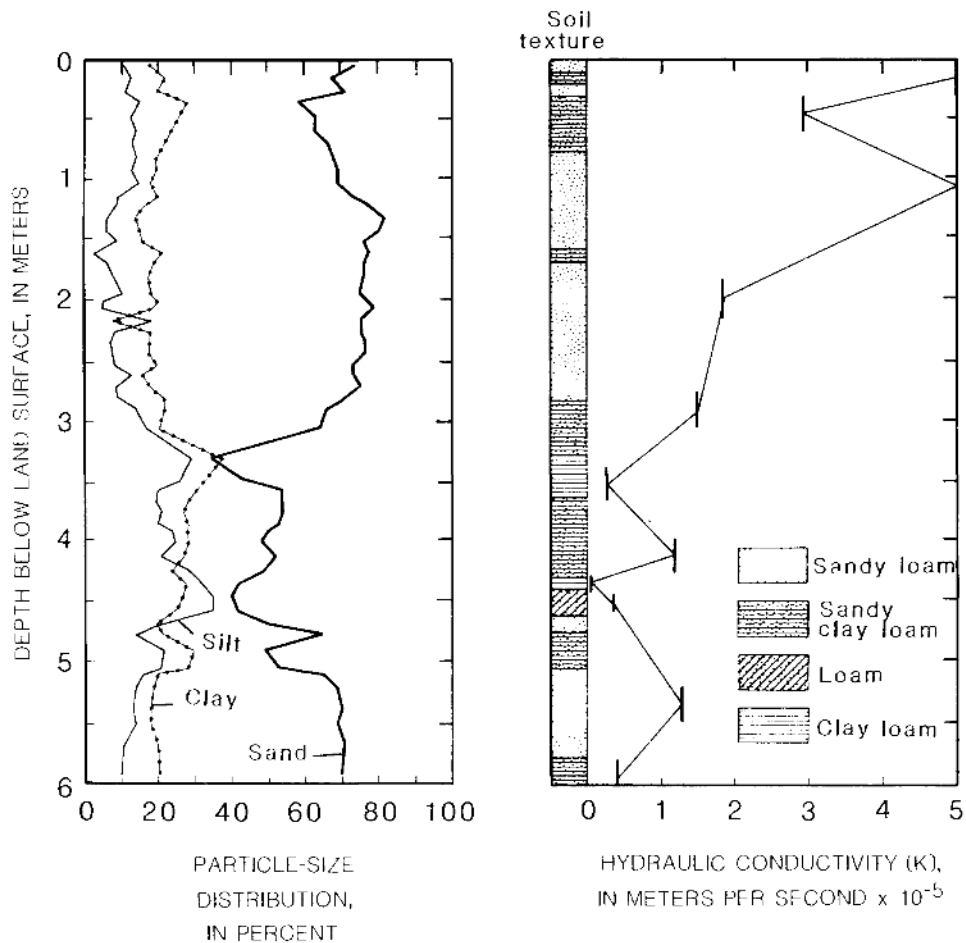
Figure 6.--Depth variation of soil-particle size, soil texture, and saturated hydraulic conductivity for Zenith site. (The vertical bars indicate that the soil sample was taken from the indicated depth interval.)

INSTRUMENTATION

The Burrton and Zenith sites exhibited favorable characteristics for recharge, including a generally sandy soil under natural grass conditions, no extensive confining clay layers, a relatively shallow water table, and a saturated zone characterized by decreasing hydraulic head with depth. Given these favorable potential-recharge characteristics, the selected sites were instrumented extensively so that direct measurements could be made of as many recharge-related characteristics as possible.

The instrumentation employed at each of the two recharge sites is diagrammed in figure 9. The purpose of the instrumentation was to provide integrated measurements that would allow calculation of subsurface flow on a year-round basis. Data collection was automated as much as possible by using battery-operated, programmable data loggers, which recorded data on magnetic tape cassettes on an hourly and daily basis at each site.

9
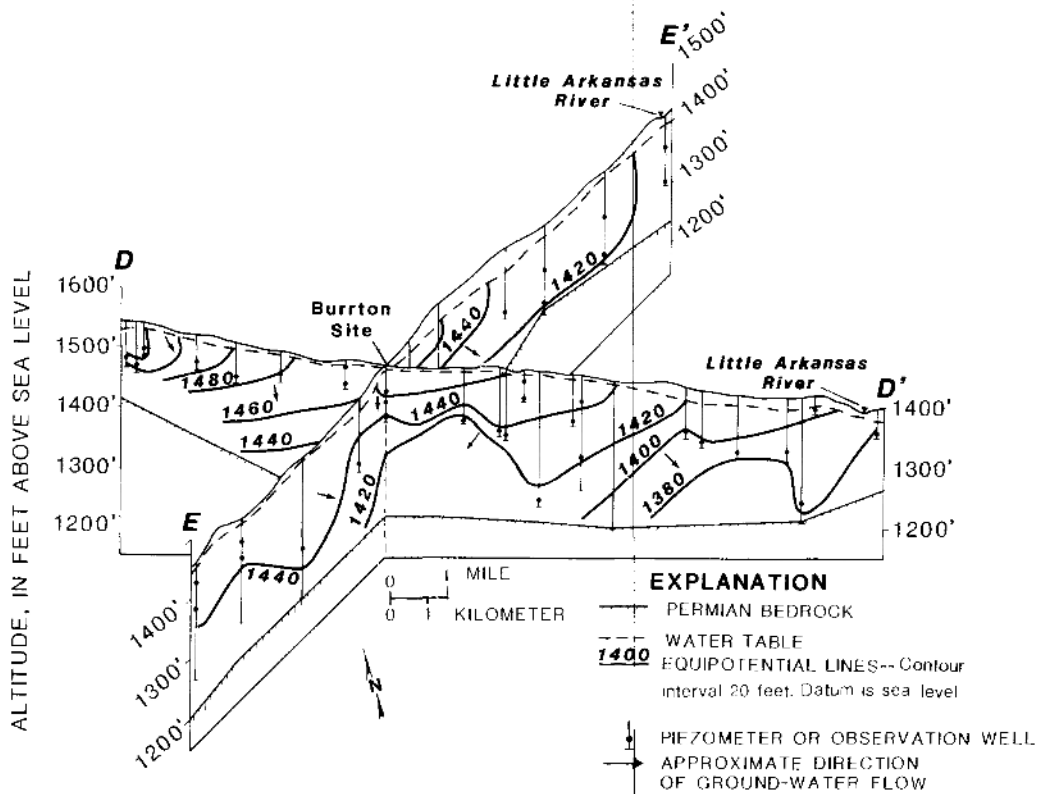
Figure 7.--Cross sections in vicinity of Burrton site depicting approximate directions of ground-water flow, 1978-81.
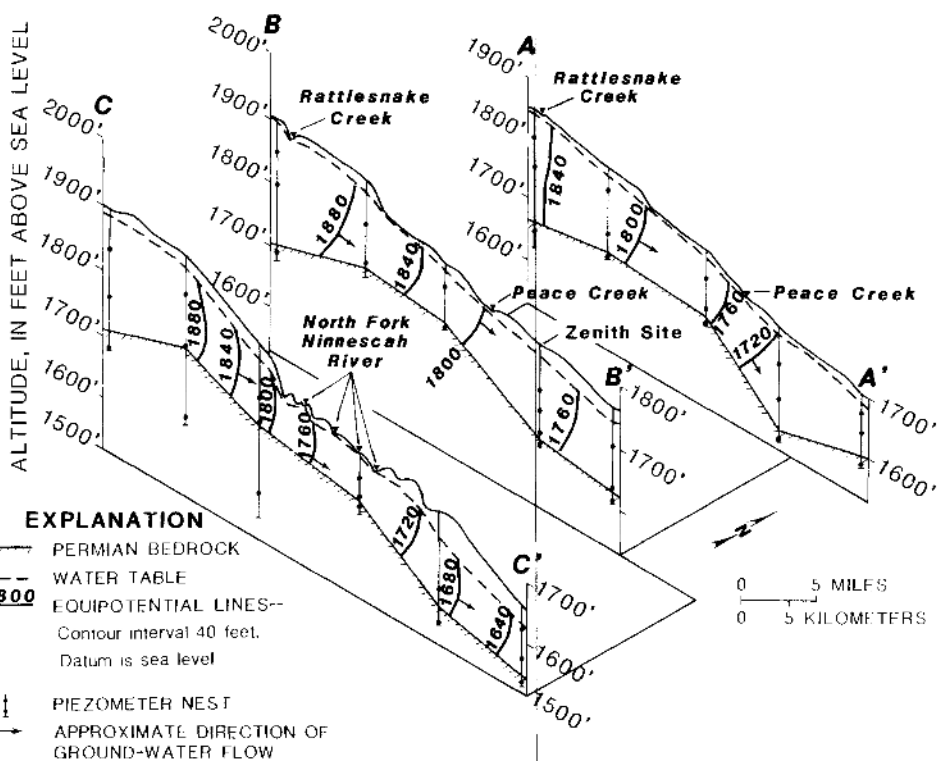
Figure 8.--Cross sections in vicinity of Zenith site depicting approximate directions of ground-water flow, 1982.

10

Through a cassette reader, these data were transferred to the office computer for processing. In addition to the automated data collection, neutron-moisture readings, as well as piezometer-nest, gypsum-block, and tensiometer readings, were made manually by observers on a weekly basis. Every effort was made to provide duplicate or alternative measurements in case some equipment malfunctioned. Both sites were instrumented during June 1982, and data collection was continued until December 1983. The onsite and laboratory measurements and the instruments or techniques used for such measurements are shown in table 1. All laboratory analyses were conducted by the Kansas Geological Survey porous-media laboratory (Lawrence, Kansas) under the direction of the senior author.

Gage houses were used to protect the electronic equipment and provided support for several of the atmospheric sensors (fig. 9). The houses were located near a utility line for 110-volt alternating-current (a.c.) power to energize the system, although the system could have operated on batteries alone. All sensor cables outside the gage house were inserted into polyvinyl-chloride pipe and buried.

NOT TO SCALE
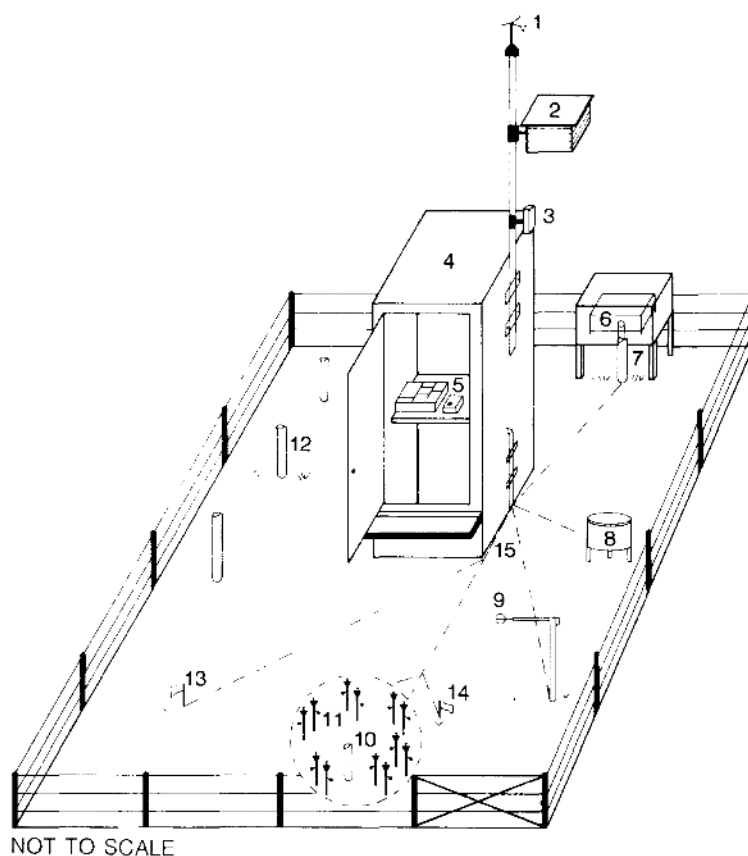
Figure 9.--Site instrumentation (1, anemometer; 2, temperature and relative humidity sensors; 3, barometer; 4, housing unit; 5, data loggers; 6, water-level recorder; 7, water-table well; 8, precipitation gage; 9, net radiometer; 10, neutron-probe access tube; 11, tensiometer nest; 12, piezometer nest; 13, thermocouple hole; 14, gypsum blocks; 15, underground connecting lines).

11

Table 1.--*Onsite and laboratory measurements*

Measurement	Instrument or technique
Onsite data - Atmospheric	
Precipitation	Tipping-bucket rain gage
Atmospheric pressure	Barometric-pressure transducer
Air temperature	Thermistor probe
Relative humidity	Lithium-chloride sensor
Wind speed	Anemometer
Net radiation	Hemispherical net radiometer
Onsite data - Subsurface[1]	
Hydraulic head	Piezometer and duplicate tensiometer nests
Water table	Water-table observation well
Soil-water content	Neutron probe, gravimetric method, and gypsum blocks
Bulk density	Gamma probe and core method
Soil temperature	Thermocouples
Laboratory data[1]	
Soil texture	Hydrometer method
Particle density	Pycnometer method
Bulk density	Clod method
Soil-water characteristic	Hanging column, pressure plate, pressure membrane
Hydraulic conductivity	Constant-head permeameter, soil-water characteristic based methods

[1] Major references: Black, 1965; American Society for Testing Materials, 1979.

Data Loggers

Data collection and storage were accomplished by microcomputer data loggers, conventional digital and graphical recorders, and observers' notes. The data loggers at each site consisted of CR-5 and CR-21 (Campbell Scientific, Inc.) units[2]. Both data loggers record data on magnetic tape cassettes that were transferred by a cassette reader (Omnidata, model 217, Datapod/Cassette Reader) to the office computer.

[2] The use of trade names in this report is for identification purposes only and does not imply endorsement by either the Kansas or the U.S. Geological Surveys.

The CR-5 data logger (fig. 10), having modular flexibility, allowed the system to be configured to drive a time-control module, digital printer, cassette interface, power supply, and a 50-channel scanner with thermocouple and 0- to 10-volt signal-conditioning cards for recording soil temperatures and soil-water pressures using pressure transducers on the tensiometers.

The CR-21 data logger (fig. 11) is a battery-powered microcomputer with a clock, a serial data interface, and a programmable analog-to-digital converter that can handle seven analog inputs and two pulse-counting inputs. Once each minute the CR-21 samples the input signals according to programs specified in a user-defined input table, processes the data, and stores them according to user-defined output programs. Programs were set to compile the collected data at both hourly and daily intervals in tables that included instantaneous data, average, total, maximum, minimum, and time of extreme event.

To facilitate wiring, an electrical-connection board was constructed (fig. 11). A ground buss bar was connected to all sensors by means of a spark gap for lightning protection.
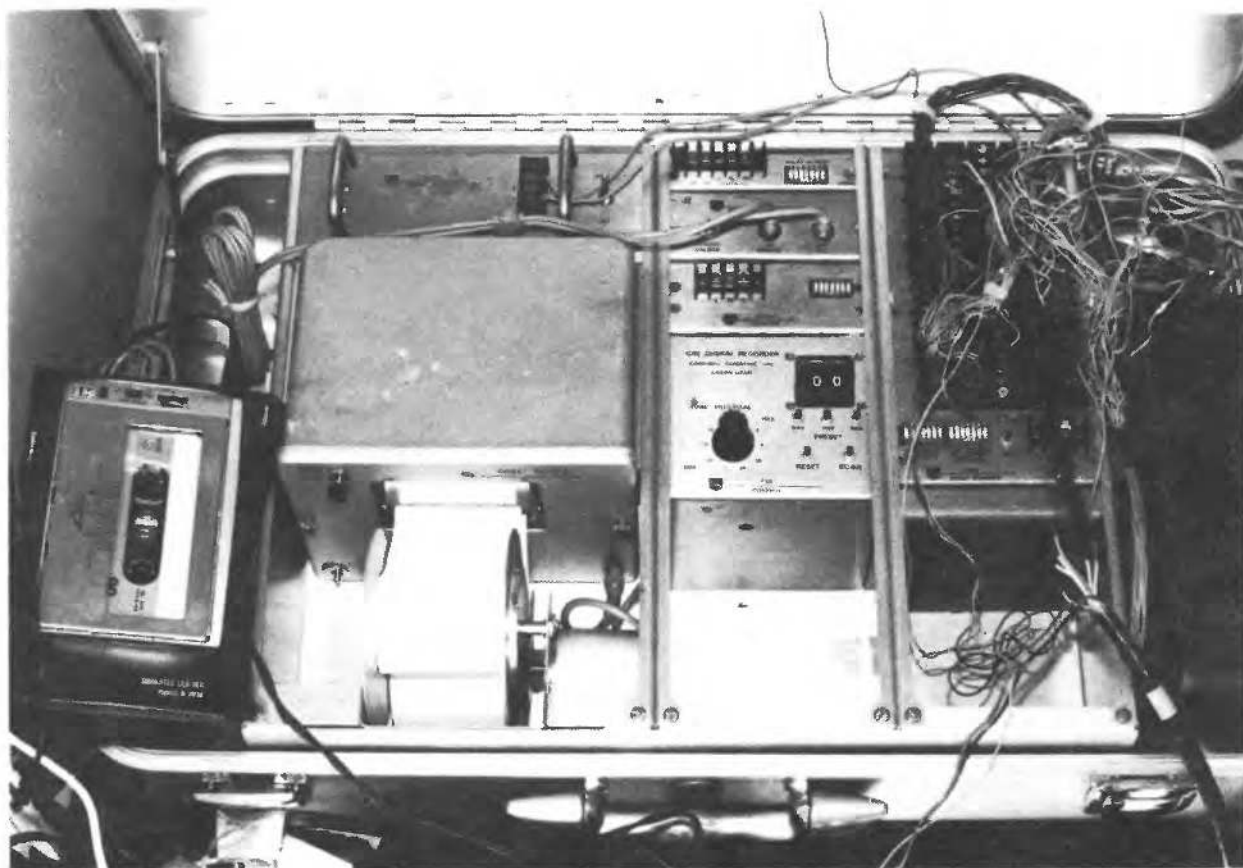
Figure 10.--CR-5 data logger and cassette recorder.

13
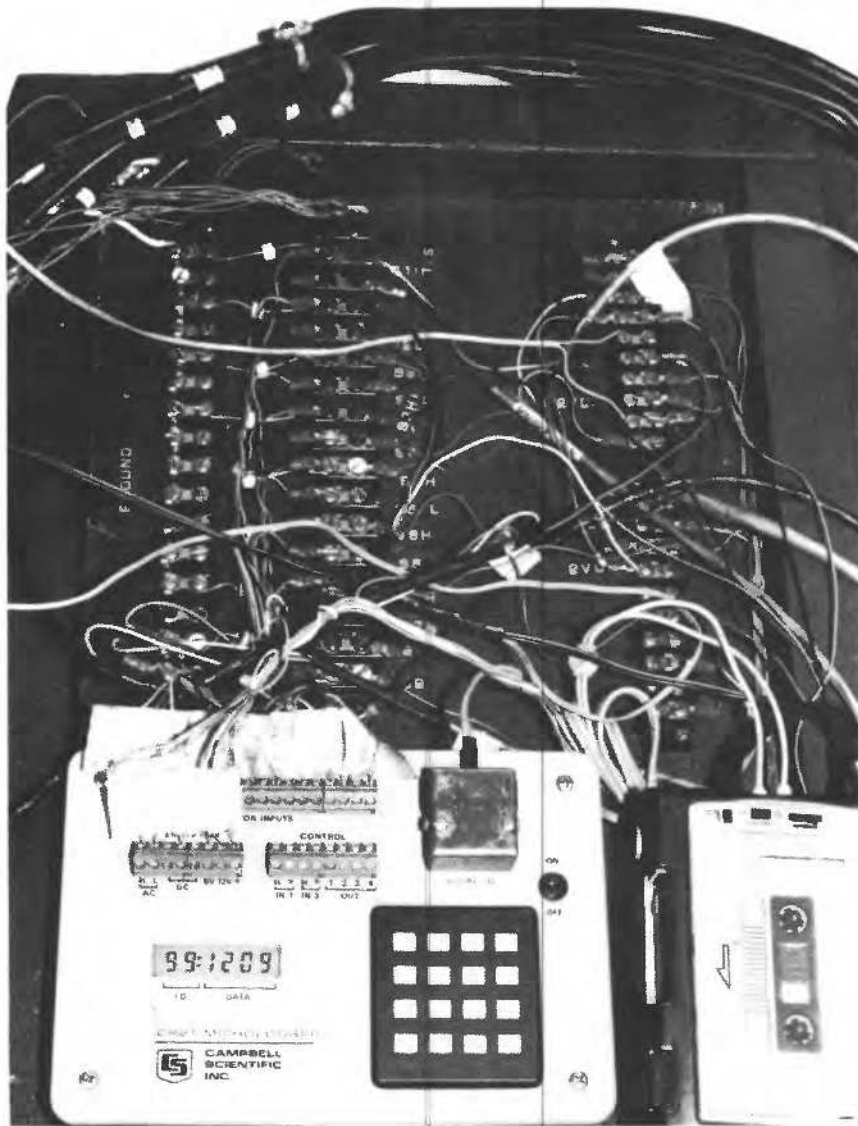
Figure 11.--CR-21 data logger with electrical-connection board and cassette recorder.

Onsite Atmospheric Data

All atmospheric sensors were connected to the CR-21 data logger, which was programmed to record hourly and daily values. A barometric-pressure transducer (Yellow Springs Instrument Co., model 2014) measured ambient site pressure. Air temperature and relative humidity were measured by the Campbell-Scientific, 201 thermistor probe and the lithium-chloride sensor. Wind speed was measured with a Met One, model 014A anenometer located approximately 4.6 m above the ground. Radiation was measured by a hemispherical net radiometer (Weathertronics, model 3032). Rainfall was measured with a Sierra-Misco model RG-2501 tipping-bucket rain gage. The rainfall data at the Burrton site were supplemented with U.S. Geological Survey rain gages, which consisted of a catchment funnel, an accumulation well, and a float connected to a Fisher-Porter paper-tape recorder.

The atmospheric sensors were checked or calibrated in the laboratory and onsite immediately after installation using mercury thermometers, a hydrothermograph (recording relative humidity and temperature), and barograph, as well as relevant data from nearby meteorological stations. Specified amounts of water were added to the tipping-bucket rain gage to check or adjust the tipping of buckets to the correct amounts of water input. From such comparative verifications, the sensors were confirmed to perform generally within the range of their specified accuracy.

Onsite Subsurface Data

Observation Wells and Sediment Lithology

Observation wells were augered to determine the depth to water and to confirm the sediment lithology. Test holes for piezometers also were augered to confirm downward flow of water in the saturated zone. Augered samples were collected for further examination and laboratory analyses (table 1). Gamma-ray logging of the deepest hole at each site (fig. 4) was conducted to confirm the sediment lithology and depths of sampling.

The piezometer nest for the Burrton site consisted of three piezometers (fig. 4), the shallowest one (P3) screened at 12 m in sand; the next (P2), at 17 m in clayey sediments above a clay layer; and the deepest one (P1), at 27 m just below a clay layer. The piezometer nest for the Zenith site consisted of four piezometers (fig. 4), the shallowest one (P4) screened at 23 m in sand; the next (P3), at 31 m in silty clay; the next (P2), at 43 m in sand and clay; and the deepest one (P1), at 48 m in red shale (bedrock). These piezometers were already in place at the start of this study as part of a ground-water-quality monitoring program.

Soil Moisture

Neutron-probe access tubes for each site were made from 54-mm outside diameter, 1.65-mm wall, cold-rolled electric-welded (CREW) hydraulic tubing; the pointed lower end was sealed with a rubber stopper and a concrete-bentonite mixture. The hydraulic tubing was pressed into a hole made by a 54-mm coring tube, resulting in a tight fit. The neutron-probe access tubes were approximately 6.1-m long and were installed to a depth just below the water table. The neutron probes used in this study were a Campbell-Pacific Nuclear, model 501 probe, with moisture and density readings, and a model 502, probe with moisture readout only. Weekly neutron readings of soil moisture were taken by observers at 0.15-m depth intervals.

The neutron probe was calibrated onsite. A 54-mm-diameter hole was drilled with a soil-coring tube and sampled continuously. The samples were sealed in plastic bags and weighted the same day. The access tube with a sealed and pointed end then was auger-pushed into the hole for a tight fit. The combination neutron-gamma probe was inserted, and moisture and bulk-density readings were taken every 0.23 m.

15

The collected core samples then were taken to the laboratory, where they were oven-dried, reweighed, and the percentage of moisture by weight determined. These samples (together with other augered samples) also were used for other laboratory soil-property analyses discussed in a following section. Using the values of soil moisture by weight and the bulk density measured with the model 501 moisture and density probe for each sample, volumetric soil-moisture percentages were determined. A correlation analysis between the sample moisture contents and the neutron-count ratios indicated a correlation coefficient of 98.5 percent (fig. 12).

Capillary Pressure

Ceramic tensiometers equipped with Bourdon dial gages and low-cost pressure transducers were used to measure soil capillary pressures. The pressure transducers sensed the negative pressure inside 12 jet-fill tensiometers (Soilmoisture, Inc., 2725 series) arranged in pairs at depths of 0.15, 0.3, 0.6, 0.9, 1.2, and 1.5 m around the neutron-probe access tube. The pressure transducers (National Semiconductor Corp., NSC, model no. LX1804GBZ) had a gage-pressure range of 0 to ± 1.5 MPa. Readings
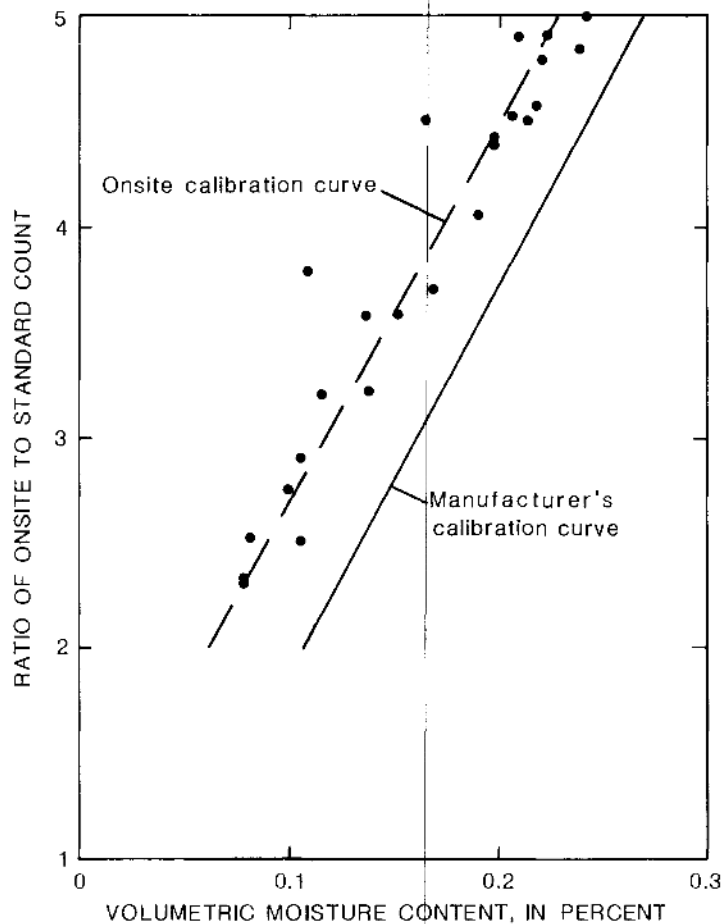
Figure 12.--Neutron-probe soil-moisture-content calibration curves.

from the 12 pressure transducers connected to soil tensiometers were taken every 3 hours through the multichannel scanner of the CR-5 data logger. A separate power supply of +12 and -5 volts and an external circuit were needed to calibrate and operate each transducer.

Tensiometer transducers were checked against their factory-stated specifications by comparison with the dial gage on the jet tensiometer. The dial gage was removed from the tensiometer, and a T-shaped brass bushing was inserted into the tensiometer gage hole. The dial gage and tensiometer transducer then were connected to each side of the T-bushing for simultaneous comparisons, and the tensiometer was inserted into a plastic container filled with wetted soil. All tensiometers also were tested in the laboratory for porous-cup conductance and response-time constants according to procedures outlined in Danielson (1982). From such comparative experiments or verifications of their factory-stated performance standard, all sensors were calibrated. The sensors generally performed within the range of their specified accuracy.

A tensiometer interface was built to convert the voltage readings from each transducer, based on its individual calibration curve, into a pressure reading. The interface (fig. 13) included a power amplifier (generic) for each tensiometer in the standard inverted configuration so that gain and offset could be adjusted independently for each tensiometer. The scaling of the transducer voltage with this interface was of great help in calibrating, checking, and readjusting the tranducer at the sites. A correlation analysis between transducer and dial-gage readings during a 2.5-month period from one of the sites resulted in a correlation coefficient of 97.8 percent (fig. 14). However, such transducers need periodic recalibration because of repeatability and stability errors (National Semiconductor Corporation, 1977; 1981).

The tensiometer-pressure transducers were calibrated at the sites by applying different tensions in each tensiometer using a hand vacuum pump and comparing the tensiometer or vacuum-pump dial reading with the cor-
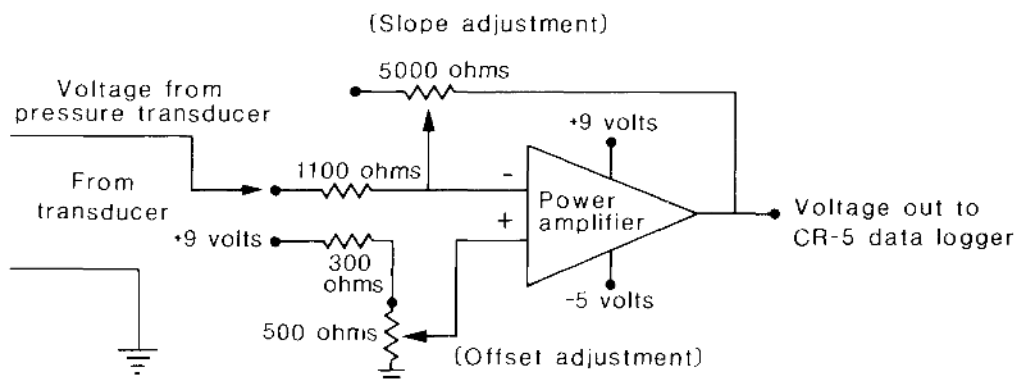
Figure 13.--Tensiometer interface designed to convert tensiometer-transducer voltage output to pressure units.

17
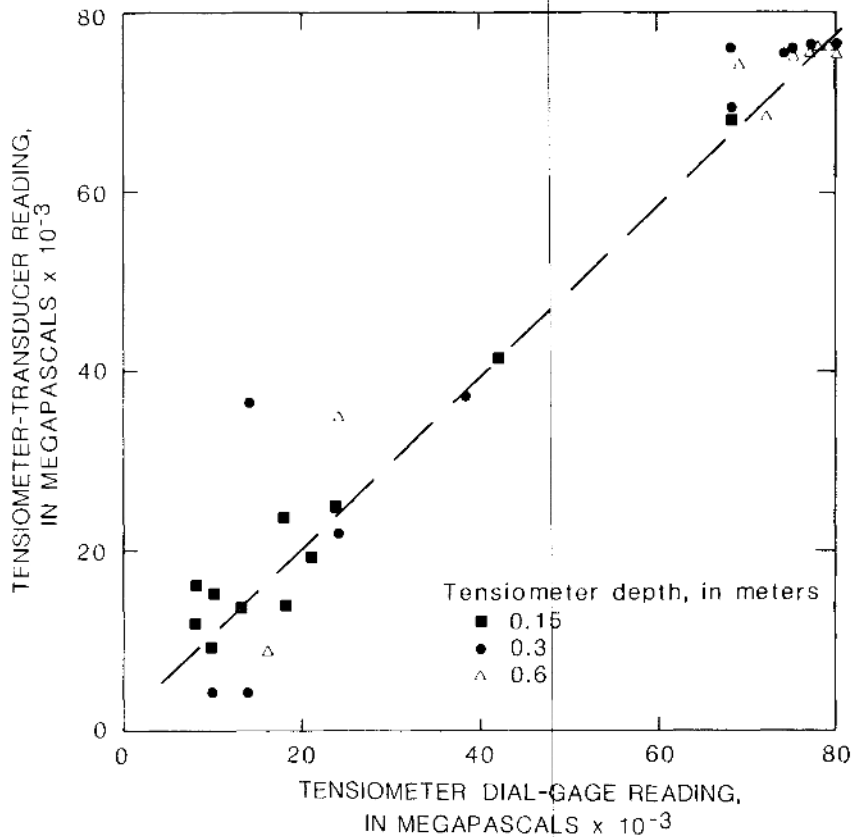
Figure 14.—Comparison of tensiometer-transducer readings and tensiometer dial-gage readings.

responding reading from the data logger. Through the constructed interface, tension in engineering units was read from the data logger. The data-logger reading was matched with the tensiometer dial-gage reading by adjusting the two interface potentiometers (fig. 13) for each transducer, one for slope and one for offset.

Ethylene glycol solution was used in the tensiometers during winter to avoid freezing and breaking. The tensiometer porous cup was saturated in the laboratory with distilled, deaerated water, and a 50-percent ethylene glycol solution was added to the tensiometer. Such tensiometers were calibrated by inserting one tensiometer filled with water and another with the glycol solution in the same soil container and comparing readings. Calibration curves between the two readings were developed with a correlation coefficient of 99.8 percent (fig. 15).

A series of gypsum blocks also were installed at various depths (after being saturated with distilled water) to supplement tensiometer data. Two Beckman gypsum blocks (model CEL-WFD) were installed at 0.3- and 0.6-m depths at each site and connected to the CR-21 data logger. All other gypsum blocks (Soilmoisture, model 5200) were read manually on a weekly basis.

18
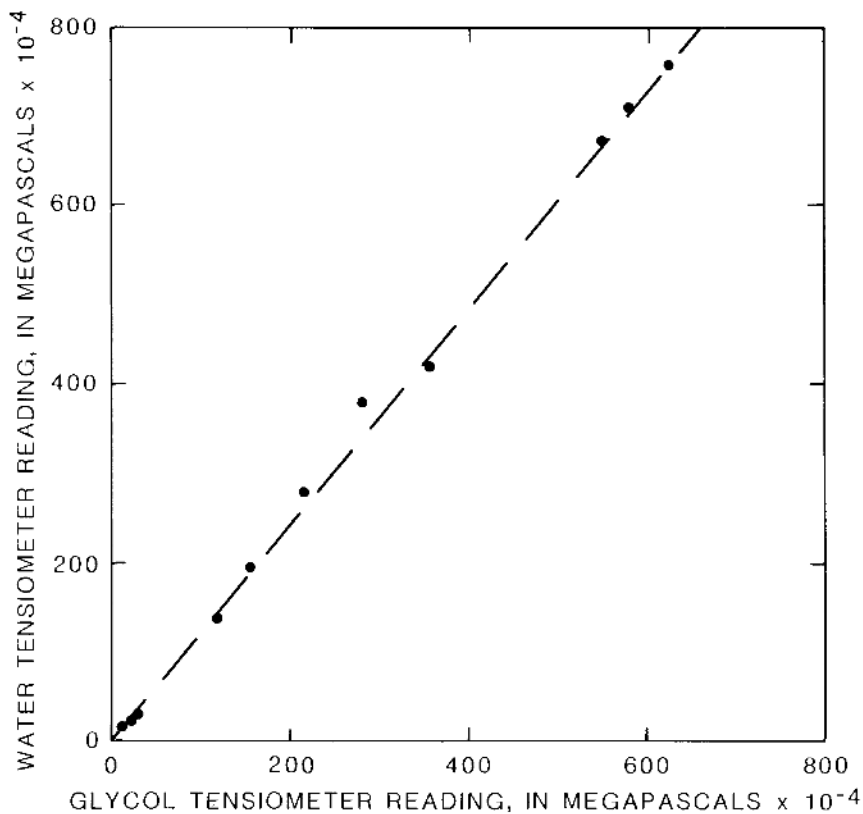
Figure 15.—Calibration curve for glycol-solution tensiometers.

Water Levels

Water levels in the water-table observation well were measured by a pressure transducer (Enviro-Labs, Inc., model PT-105V). A voltage divider was needed to connect this pressure transducer to the CR-21 data logger. The water-level transducer was inserted into a pipe filled with water to check the indicated height of the water column above the transducer.

The water-level pressure transducer also was calibrated at the sites by inserting it in the water-table observation well to a certain depth below the water table and raising it upwards by small increments, while at the same time taking the corresponding voltage readings from the data logger. From a regression analysis of pressure-transducer positions in the water-table observation well and corresponding voltage readings, a slope and offset were obtained, which were programmed into the CR-21 memory so that the water level was read directly from the CR-21 data logger. An alternative method of measuring ground-water levels consisted of a conventional float gage with a Stevens type-A graphic-stage recorder. This recorder was connected by a chain drive to a variable potentiometer, which in turn was connected to the CR-21.

Water levels in all other observation wells at the sites (as well as in the water-table observation wells) were read manually on a weekly basis using a steel tape. Water levels in nearby observation wells also were read using a steel tape, but on a monthly basis.

19

Soil Temperature

Readings from 15 soil-temperature thermocouples at various depths, spaced in a geometric progression from near ground surface to 7.6 m below land surface were taken every 3 hours using the multichannel scanner of the CR-5 data logger. The soil-temperature thermocouples were made from wires of copper and constantan (Omega Engineering, Inc., PR-T-24). The junctions of the dissimilar metals were protected from corrosion by coating them with an epoxy with good thermal conductivity and electric insulation (Omegabond 100 from Omega Engineering, Inc.). The thermocouple wires and junctions were attached, at the proper spacing, to a heavy, stiff, and well-insulated wire, which was inserted into an augered hole. The hole was backfilled carefully with the same augered material so as to maintain good contact between thermocouple junctions and the soil. The copper-constantan thermocouples were checked in the laboratory against mercury thermometers and generally found accurate within their specifications.

Laboratory Determination of Soil Properties

Soil samples were collected during observation-well and neutron-access-tube installation and analyzed in the laboratory for the properties shown in table 1 to supplement and check the data collected onsite. The unsaturated hydraulic conductivity as a function of soil-water content was determined using water-characteristic or desaturation curves in combination with saturated hydraulic conductivity by employing a number of hydraulic-conductivity function-prediction techniques as will be detailed in the methodology section. The soil-water characteristic curves were determined using the hanging-column method for low pressures up to -0.025 MPa, the pressure plate apparatus for up to -0.5 MPa, and the pressure membrane apparatus for up to -1.5 MPa (table 1). The saturated hydraulic conductivity was measured using the constant-head method (table 1).

INSTRUMENTATION PROBLEMS AND SUGGESTIONS FOR IMPROVEMENT

Reliable onsite measurements can be achieved by using properly designed and calibrated instruments in combination with careful installation involving minimal soil disturbance. However, even with appropriate precautions, many difficulties occur in assuring long-term accuracy.

Tensiometer System and Gypsum Blocks

Air leaks and bubbles that occur in the tensiometers as they are placed under a partial vacuum for long periods, along with temperature and humidity affects on both tensiometers and transducers, caused difficulties in obtaining long-term measurements of matrix potentials. Other problems included difficulties in maintaining physical contact with the soil,

20

especially with disruptions caused by repeated servicing and recalibrations required for the tensiometer transducers and by plant roots that tend to grow around the base of the tensiometers. Persistent problems occurred with the tensiometer transducers, which are extremely sensitive to moisture. Moisture contacting the transducers resulted in corrosion and failure. Despite extraordinary measures taken to protect them, such as spraying with a moisture-resistant lacquer, taping with water-resistant tape, covering in plastic bags, and protecting the tensiometer-transducer system with inverted plastic buckets, most transducers eventually failed. Another pressure transducer with moisture-resistant coating (National Semiconductor Corp., model LX1804GBZ-1) also was tried, but the problems persisted. Nevertheless, backup measures, such as installation of two tensiometers for each depth and connection of a dial gage in addition to the transducer in each tensiometer, allowed a long period of tensiometric readings.

Although ethylene glycol-filled tensiometers performed well during winter, the Bourdon-type dial gages (Soilmoisture, Inc., model 2060G2) connected to the tensiometers were sensitive to freezing conditions, and some became ineffective after freezing. In general, several such dial gages deteriorated with time, and moisture accumulated within the dial gage.

With regard to the gypsum blocks, it is well known (Gardner, 1965) that they are low-precision instruments. In addition, these blocks proved rather insensitive to moisture-content changes in the wet range of soil-moisture content. However, the gypsum blocks that were recorded continuously through the CR-21 data logger proved useful in indicating significant moisture-content changes from dry to wet conditions and vice versa, and thus useful in tracing sharp moisture-front movement as will be shown in a later section.

Water-Level Pressure Transducers

Another problem occurred with the water-level pressure transducer connection to the data logger. Because the CR-21 data logger accepts a maximum signal of 2.5 volts, while the water-level pressure transducer emits a maximum signal of 5 volts, a voltage divider was built and connected to the transducer cable before connecting it to the CR-21. Graphical displays of the resulting measurements indicated an unusually pronounced fluctuation cycle, very similar to the diurnal temperature cycle. Fluctuations of temperature of the air and the interior of the housing unit showed similar patterns. The voltage-divider resistors were temperature sensitive, thus affecting the measurements. This was checked by heating the voltage divider and observing the corresponding changes in the CR-21 output. However, daily averages of hourly water levels closely matched the manually measured weekly water-table readings. To avoid any further problems related to the temperature sensitivity of the voltage-divider resistors, the water-level pressure transducer was connected directly to the CR-5 data logger, thus resolving the problem. This data logger, however, produced voltage readings that needed to be converted to water levels.

In addition to the problem with temperature sensitivity of the voltage divider, the pressure transducer failed a number of times. To avoid loss of data, a backup system consisting of a Stevens graphic-stage recorder in combination with a potentiometer was calibrated to electrically indicate the water level on the CR-21 data logger.

Direct-Current Power Supplies

A 12-volt lead-acid battery was used for the CR-5 and CR-21 power supply to provide the extra current needed to operate the pressure transducers. Great care was taken to avoid any cross connections that could drain the internal batteries of the data loggers. As commercial power was available at the sites, a battery charger was installed and programmed by the CR-21 data logger to charge the battery for an interval before the hourly readings were taken. Initially, a charging time of 15 minutes was set. However, with the advent of colder temperatures, this preset time was inadequate, and the battery was undercharged on several occasions. Thus, for winter operations, the charging time was increased from 15 to 25 minutes before the hourly readings. During cold weather the cassette recorders also were sluggish, and some data were lost. These problems were solved temporarily by using thermostatically controlled heating units to maintain housing temperature at a nearly constant level. However, because of repeated battery problems, the batteries were replaced with alternating-current (a.c.) power supplies.

Data Loggers

The major problem with the data loggers was the protection from extraneous voltage supplies and static electricity. The spark gaps are sufficient for normal, dry-weather static electricity but are not protection enough for nearby lightning strikes. Both data loggers at the Zenith site had to be returned to the factory for major repair after a lightning strike. Care must be taken also when connecting the various sensors and to guard against any cross connections between earth ground and the "low" side of the analog input channels of the CR-21. Any voltage larger than 1-volt direct current (d.c.) above the earth ground connected to the low side resulted in erratic readings from the other sensors.

Internal batteries (if not rechargeable) should be removed before applying external power, or else they may explode due to inadvertent recharging. A minor problem with the transfer of data to the computer was encountered because the tape-recorder heads were not positioned exactly alike. To get the best transfer of data from audio signal on the cassette to the computer-disk file, the following adjustments were made to the recorder that was connected to the cassette reader. First, the data cassette was played while the adjustment screw on the recorder head was turned until the audio signal was loudest and most crisp. Then, the connecting cables were connected to the interface, and the data transferred to the computer.

Suggestions for Improving Instrument Performance

As a result of experiences gained during this investigation, several suggestions are offered to enhance the reliability of the data-collection system and to minimize data losses.

(1) Purchase sensors and data loggers from reputable firms with long histories of established performance.

(2) Arrange backup systems in case of failure of one sensor or data logger. An additional data logger, for example, will recover its cost over the long term.

(3) Obtain electronic equipment and sensors with built-in shock and polarity protection, or install such protection before use. This is especially important with pressure transducers, which may be destroyed by reverse connections.

(4) Have available the services of a well-trained electronic technician. Also, carefully train the onsite observers in the servicing of equipment and in the recognition of problems.

(5) Establish two-way radio or telephone communication between distant sites and headquarters.

(6) Obtain sensors with output compatible to the data-logger input requirements so that no additional electronic components are needed.

(7) Insulate the unit housing, the data loggers, and all electrical connections against moisture and temperature fluctuations as much as possible.

METHODS FOR ESTIMATING GROUND-WATER RECHARGE

Determination of Vertical Soil-Water Fluxes

The customary method of calculating ground-water recharge by multiplying a constant specific-yield value by the water-table rise over a certain time interval may be erroneous. Error can be introduced if regional ground-water inflow and outflow are not considered, if ground-water losses attributed to pumpage or stream base flow are not properly accounted, or if properties of the unsaturated zone are not considered (Duke, 1972; Sophocleous, 1985). Therefore, vertical water fluxes were calculated by employing Darcian approaches in combination with water-balance equations as described in the methods below:

(1) The vertical hydraulic gradient was measured based on tensiometer readings and multiplying that gradient by the corresponding unsaturated hydraulic conductivity. However, because of hysteresis effects and frequent tensiometer malfunctions, this method was used only for providing support in questionable cases or for backup data for filling in gaps when using method 2.

23

(2) An "average" onsite water-characteristic curve, $\psi(\theta)$, was obtained from concurrent tensiometer and neutron readings for certain depth intervals. The hydraulic gradient then was determined from that curve by determining the hydraulic-head values corresponding to the measured neutron-moisture contents, θ, at the required depths. Finally, that gradient was multiplied by the appropriate hydraulic-conductivity function, $K(\theta)$, to obtain the water flux at the required depth interval. The average soil-water-characteristic curve is found advantageous over direct tensiometer readings for several reasons: (a) it averages hysteresis effects, since it is the mean of the wetting and drying curves; (b) it avoids tensiometer failures due to leakage, freezing, and so forth, and (3) neutron readings, upon which this method is based, are more reliable for a long-term record than are tensiometer readings. The $K(\theta)$ function, in turn, was estimated based on the saturated hydraulic-conductivity value and the water-characteristic curve. For this purpose, several already well-established procedures were employed, such as those of Millington and Quirk (1959; 1961) and Brooks and Corey (1964), as will be discussed later.

(3) However, both methods 1 and 2 could estimate only the soil-water fluxes up to the depth of the deepest tensiometer; that is, up to 1.2 m at Burrton and 1.5 m at Zenith. In order to obtain the water flux at the water table for the case where the water table was significantly below the depth of the deepest tensiometers, a water-balance equation for the soil profile was employed. This procedure is based on periodic moisture-content measurements along the soil profile (Rose and others, 1965; van Bavel and others, 1968). From the one-dimensional (vertical) form of the water-balance equation

$$\frac{\partial \theta}{\partial t} = - \frac{\partial q}{\partial z} ,$$ (1)

assuming negligible lateral soil-moisture flow, one obtains by integration from depth z to depth z+dz:

$$q_z = q_{z+dz} + \int_z^{z+dz} \frac{\partial \theta}{\partial t} dz ,$$ (2)

where q_z is the vertical component of the Darcian water flux (meters per day--positive in the upward direction); θ is the volumetric water content (cubic meter of water per cubic meter of soil); and t is time (days). A computer program was written to solve equation 2 by dividing the unsaturated zone (land surface to the water table) into N layers of thickness, Δz_i. The most critical aspect in applying this procedure is that the water flux at a particular depth must be known, and this may not be easy to determine.

To avoid this difficulty, the zero-flux plane method was employed (Kimball and Jackson, 1975). This method is based on locating the point of zero hydraulic gradient and thus the zero reference flux in the soil profile, and then summing up the changes in water content above or below

24

that point. However, this method has the disadvantage in that, during periods of significant recharge, the hydraulic gradient is not zero anywhere in the unsaturated profile, as can be seen in figure 16. Thus, the zero-flux plane method could not be used under these conditions. Therefore, the Darcian flux, based on method 2 described earlier, was used as the reference flux in applying the water-balance equation (2) to calculate the flux at the water table for the Zenith site. For the Burrton site, equation 2 was not employed because the shallow depth to the water table was within the range of the tensiometers.

Soil-Water Characteristics or Moisture-Retention Curves

The two fundamental relations that are characteristic for any given soil and are required for the calculation of soil-water fluxes are the soil-water characteristic, $\psi(\theta)$, and the hydraulic-conductivity, $K(\theta)$, functions. Laboratory determinations and onsite observations of simultaneous tensiometer and neutron-probe-based soil-moisture readings were used to develop soil-water characteristic curves.

An example of a laboratory-determined moisture-retention curve for a disturbed sample from the top 0.3 m of soil at the Zenith site, together with onsite-measured pairs of neutron-moisture and tensiometric pressure-head values, is shown in figure 17. Similar laboratory-derived moisture-retention curves were determined for a number of soil samples from different depths at each recharge site. The tensiometer data scatter is significant, and the range of tensiometer measurements is limited to greater than -0.1 MPa pore pressures. Because of the unconsolidated and disturbed nature of most samples and because of the vacuum-saturation method used to saturate the samples in the laboratory, the estimated

HYDRAULIC HEAD, IN METERS

EXPLANATION

A   PROFILE DURING NONRECHARGING PERIOD

B   PROFILE DURING RECHARGING PERIOD
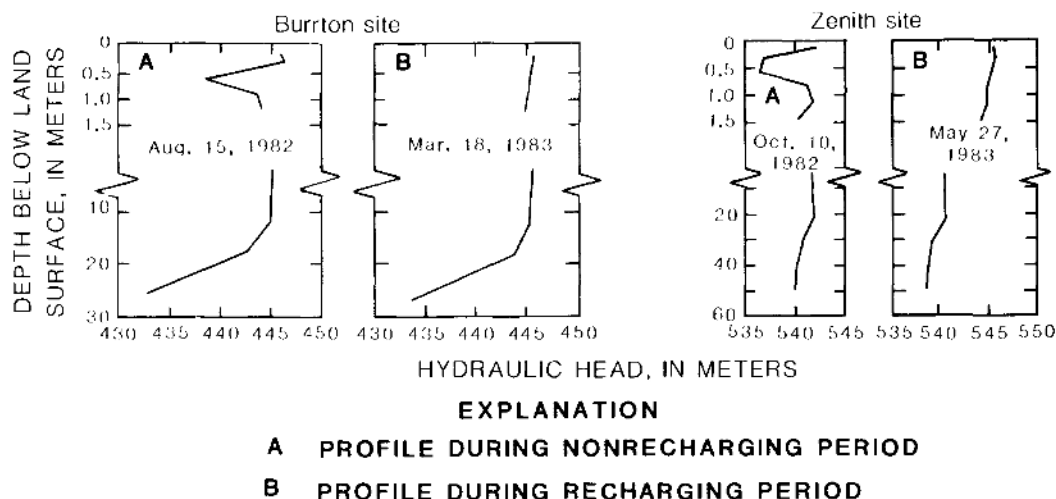
Figure 16.--Hydraulic-head profiles for nonrecharging and recharging periods at Burrton and Zenith sites.

complete water saturation was greater than the maximum observed water content measured at the site using the neutron probe. However, the agreement between laboratory and onsite measurements, considering all measurement errors and hysteresis effects as well as the disturbed nature of the samples, was considered to be satisfactory.

Onsite water-characteristic curves developed for the deepest tensiometers, such as those at 1.2 and 1.5 m at the Zenith site, are shown in figure 18 and are used to calculate hydraulic gradients for use in determining the reference flux in a water-balance equation that estimates flux at the water table, as was explained in the section on "Determination of Vertical Soil-Water Fluxes." Notice that the range of tensiometer readings is limited and that the empirically fitted curves are only a rough approximation of the true curve, due to data scatter. Given the large width of the soil-water characteristic envelope curve at the site (fig. 18), such water fluxes should be considered approximate estimates.

EXPLANATION

PRESSURE HEAD

● Pressure head from 0.3-meter onsite tensiometer

■ Pressure head from 0.15-meter onsite tensiometer

○ Pressure head from laboratory desaturation experiments
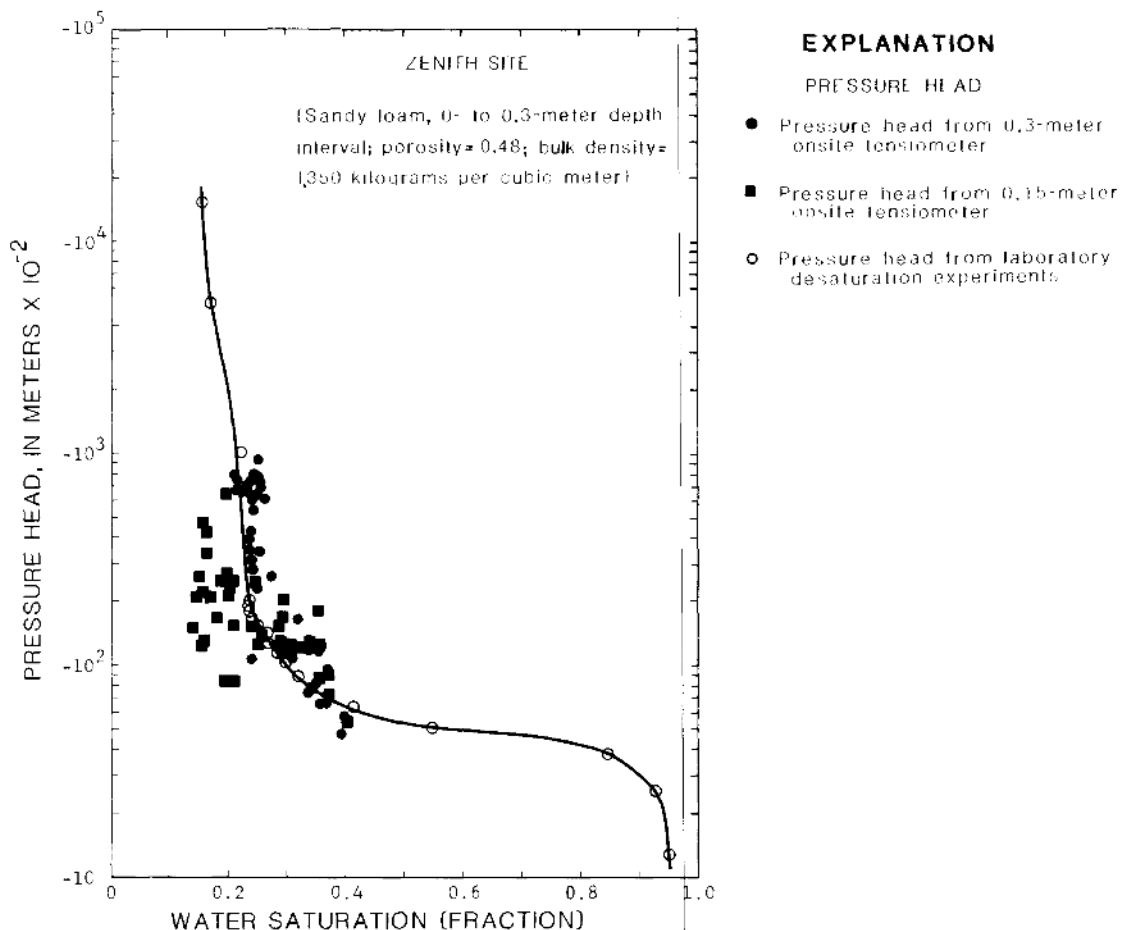
Figure 17.--Comparison of onsite- and laboratory-determined capillary pressure-head measurements for top 0.3 meter of soil at Zenith site.

26

EXPLANATION

WATER CHARACTERISTIC CURVES

Envelope curve encompassing
measured 1.2- and 1.5 meter
tensiometer-dial readings

—— Mean curve for 1.5-meter
tensiometer-dial readings

---- Mean curve for 1.2-meter
tensiometer-dial readings

■ TENSIOMETER READING
AT 1.2-METER DEPTH

● TENSIOMETER READING
AT 1.5 METER DEPTH
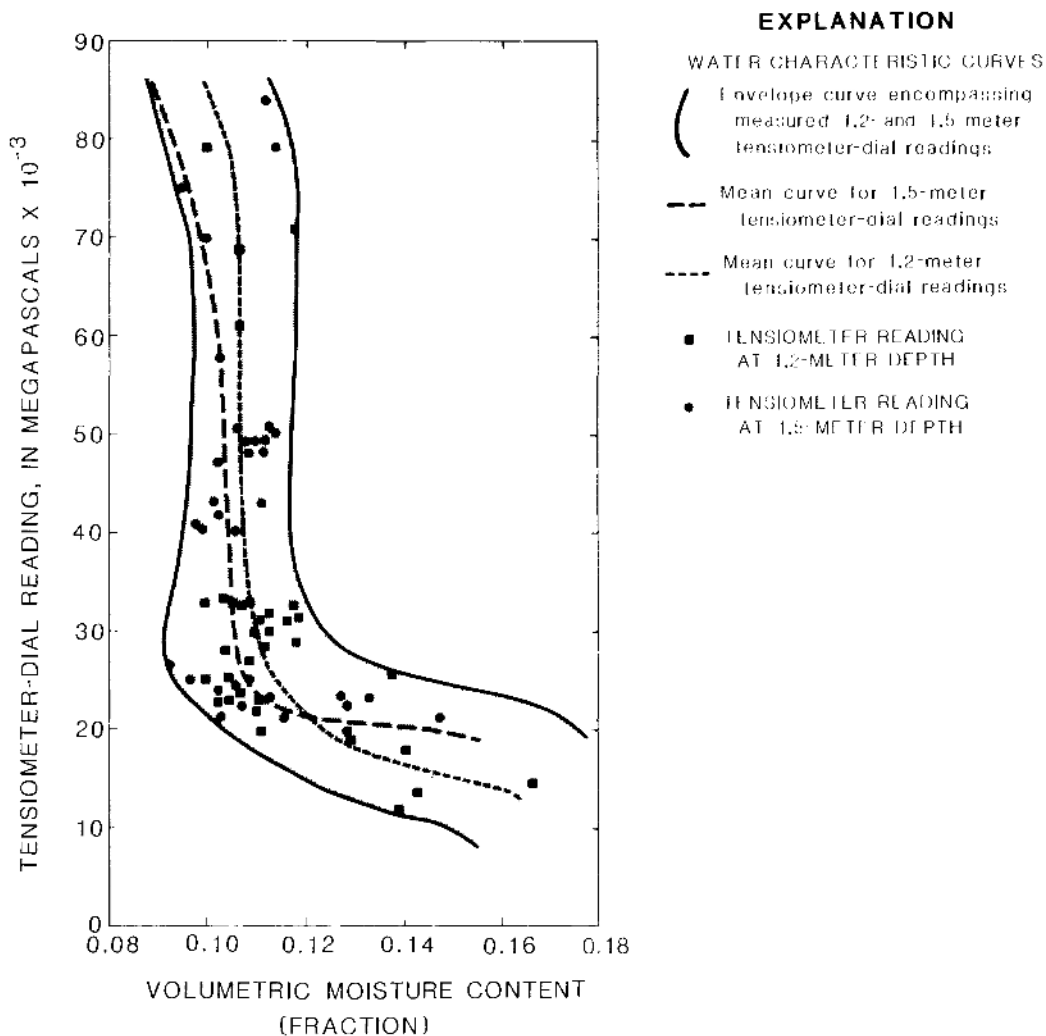
Figure 18.—Soil-water characteristic curves for 1.2- and 1.5-meter levels
at Zenith site.

Hydraulic-Conductivity Function

Application of the previously mentioned methods for calculating vertical water fluxes depends on the success of accurately determining the hydraulic-conductivity function, $K(\theta)$, which is one of the most difficult recharge characteristics to determine directly at a site. In addition, the $K(\theta)$ function is one of the most spatially variable characteristics (Warrick and Nielsen, 1980), compounding the measurement problem. To overcome some of the estimation problems, a number of techniques to predict the $K(\theta)$ function were used. These techniques are based on easily measured recharge characteristics, such as saturated hydraulic conductivity and soil-water characteristic curves.

Because of the unconsolidated nature of the sandy deposits, continuous, undisturbed core samples could not be obtained from either recharge site. Therefore, all soil analyses were performed on disturbed samples, which were compacted to onsite bulk density as determined using the combination neutron-density probe. A computer program reported by Nielsen and others (1973) was modified for calculating the $K(\theta)$ function using four methods developed by the following: (1) Childs and Collis-George, 1950; (2) Marshall, 1958; (3) Millington and Quirk, 1959; 1961; and Jackson and others, 1965; and (4) Kunze and others, 1968. A fifth method developed by Brooks and Corey (1964) was added to the program (Shaukat and Sophocleous, 1983). Sixteen pore classes, obtained by dividing the soil-water characteristic curve into a number of volumetric-moisture and pressure-head intervals, were used for all such determinations.

Evaluation of the five different methods versus measured data from the literature (Shaukat and Sophocleous, 1983) indicated that the Brooks and Corey (1964) method most closely approximated the measured values. Therefore, the Brooks and Corey (1964) method was adopted in this study. The fact that the soils at the recharge sites are sandy makes the choice of the previously mentioned capillary flow-based approaches, such as the Brooks and Corey method, appropriate for calculating the $K(\theta)$ function. Also, the fact that the $K(\theta)$ function is used to calculate reference fluxes at some appreciable soil depth (1.2-1.5 m), where the observed moisture contents were not as dry as the near-surface soils, makes the estimation of the $K(\theta)$ function approach more meaningful.

Examples of hydraulic-conductivity functions, $K(\theta)$, determined by the five different methods, are shown in figure 19. Soil $K(\theta)$ functions in figure 19a correspond to locations near or at the water table during recharge periods at the Burrton site, while the ones in figure 19b correspond to the deepest tensiometer depths at the Zenith site. Note the large decrease in unsaturated hydraulic conductivity with a small decrease in soil moisture. The horizontal segment in the Brooks and Corey curves represents the fact that the water saturation corresponding to the air-entry pressure [derived by trial and error according to the Brooks and Corey (1964) technique] is appreciably different from complete water saturation, corresponding to zero capillary pressure for these particular samples. The Brooks and Corey method is based on the assumption that the hydraulic conductivity at capillary pressures less than or equal to the air-entry pressure is equal to the saturated hydraulic conductivity. This explains why the Brooks and Corey curve is horizontal for the range of moisture content corresponding to the range from air-entry pressure to zero capillary pressure (full saturation).

For the Burrton site, the average volumetric moisture at a depth interval of 0.3-0.9 m (which corresponds to the average depth to the water table during March to July 1983) was approximately 22 percent. This soil moisture corresponds to a value of unsaturated hydraulic conductivity of 6.5×10^{-4} m/d using the Brooks and Corey curve (fig. 19a). Because the average soil-moisture content at the depth interval of 1.2-1.5 m (which corresponds to the depth of the deepest tensiometers) was about 12.4 percent for the Zenith site during March to June 1983, the Brooks and Corey $K(\theta)$ curve for that depth (by extrapolating fig. 19b by more than one
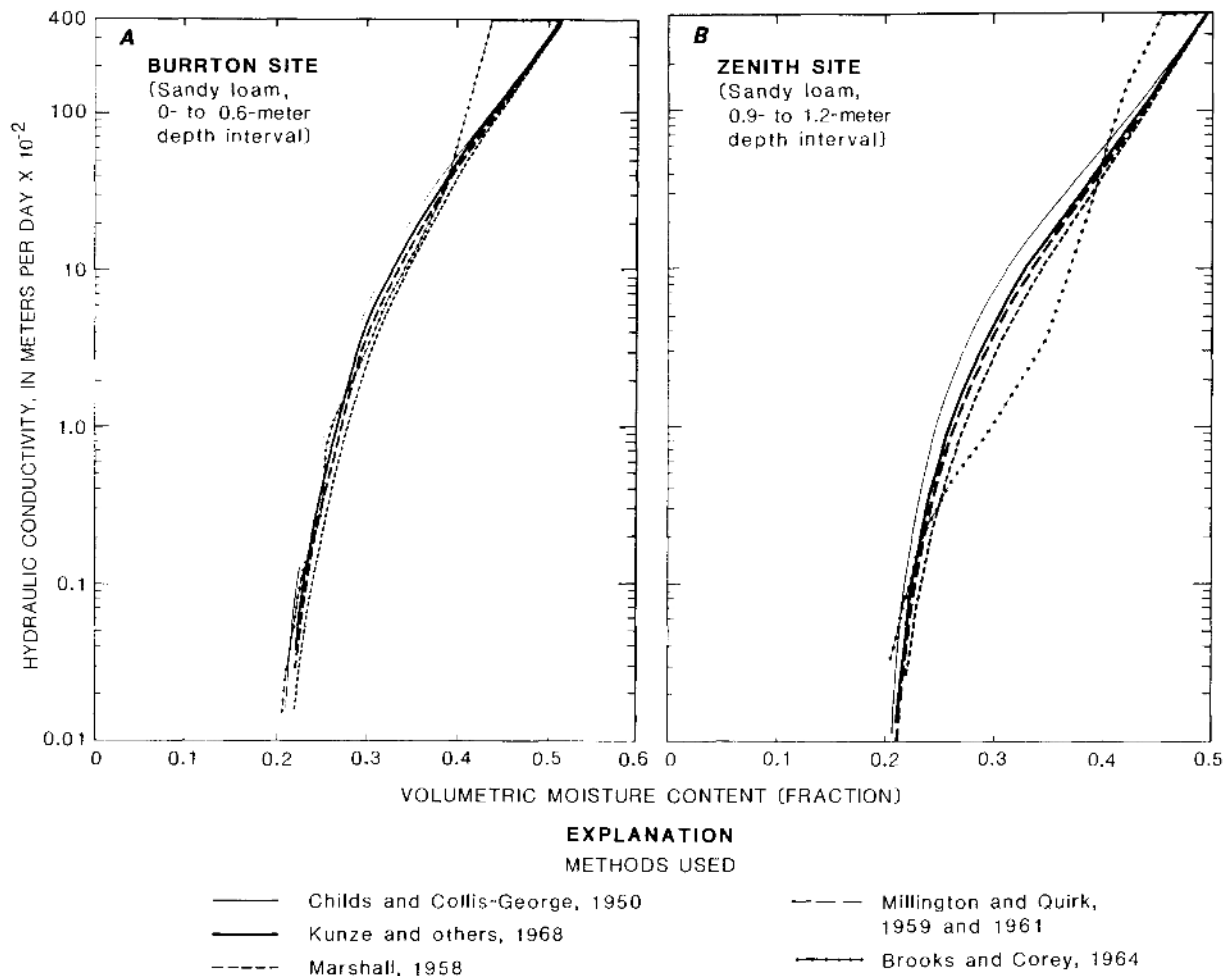
Figure 19.—Hydraulic-conductivity functions estimated using five different methods for (a) Burrton and (b) Zenith sites.

log cycle) resulted in an unsaturated hydraulic conductivity of 3.0 x 10^{-6} m/d. This large difference in unsaturated hydraulic conductivity between the two sites will result in significant water-flux differences in those depth intervals as will be shown in the next section.

Potential Evapotranspiration

Potential evapotranspiration (PET) at the recharge sites was estimated to better explain observed moisture distributions in the soil profile during different time periods, especially the occurrence or nonoccurrence of recharge, as well as its relative amounts. PET was calculated using the combination methods of Penman (1948; 1963) and of van Bavel and Businger (van Bavel, 1966; Businger, 1956) and the radiation method of Jensen and Haise (1963; see also Jensen, 1966; Jensen and others, 1970). In a comprehensive comparison of measured and estimated evapotranspiration values using 16 different methods, it was concluded

29

(Jensen, 1973) that for inland, semiarid environments the van Bavel and Businger method (with a roughness parameter of $z_o = 2.5$ mm) and the Jensen and Haise method provided the best estimates of PET, while the Penman method provided the next-best estimate.

Because net radiation was measured at the recharge sites, a correlation was determined between the measured net radiation and total solar radiation measured at the Sandyland Experiment Station (25 km west of the Zenith site, fig. 3) for use in the Jensen and Haise method. The linear regression equation developed using a sample of 126 daily values is as follows:

$$R_s = 92.2750 + 1.4003 R_n, \tag{3}$$

where R_s (langleys per day) is the total solar radiation, and R_n (langleys per day) is the net radiation. This linear regression equation has a correlation coefficient of 0.86.

A computer program was written to solve the potential-evapotranspiration equations listed in table 2. All PET estimates from the equations in table 2 were calculated in langleys per day and then converted to equivalent depth of evaporation by assuming that the latent heat of vaporization of water is 585 cal/gm. The daily soil-heat flux, G, was considered negligible in this study because it is usually quite small, and it tends to average out over a 24-hour period.

Comparison of potential-evapotranspiration estimates using the combination and radiation methods mentioned previously showed that for both sites the Jensen and Haise evapotranspiration estimates were mostly smaller than the Penman and the van Bavel and Businger estimates, both of which were reasonably close to each other, as shown in figure 20. The reason for the closeness of the Penman and the van Bavel and Businger estimates lies in the fact that both formulations are similar in that net radiation and wind effects (equations 4 and 5 of table 2) are explicitly taken into account, while the Jensen and Haise estimate does not explicitly consider wind effects. The more rapid the wind speed, the larger the observed discrepancy is between the Jensen and Haise estimate, on the one hand, and the Penman and the van Bavel and Businger estimates, on the other.

GROUND–WATER–RECHARGE ESTIMATES

Burrton Site

The ground-water-recharge profile, which includes the effective recharge period of February 10 (Julian day, JD41) to May 27 (JD147), 1983, for the Burrton site, is shown in figure 21. During parts of this period, the data logger, which stored the hydrologic and meteorological data for the site, failed. Therefore, the average total precipitation data from six nearby meteorological stations (shown in fig. 3) were used for the Burrton site. The distribution of total precipitation during various

30

time intervals between site visits is shown as a bar graph (fig. 21a).
The resulting volumetric moisture content at 0.3-m-depth intervals for the
upper 0.9 m of soil is shown in figure 21c. The moisture content at the
0.9-m depth from April to July 1983 approaches the saturated water content
for that depth because the depth to the water table was less than 1 m
during the period. The moisture storage integrated at 0.15-m intervals
for the soil profile from the land surface to 2.0-m deep is shown in figure
21d. This total assumes that the moisture content at 0.15 m is represent-
ative of the layer from the land surface to 0.23-m deep, the 0.30 reading
is representative of 0.23 to 0.38 m, and so forth.

Table 2.—*Evapotranspiration equations*

$$ET_P = \frac{\Delta}{\Delta+\gamma}(R_n + G) + \frac{\gamma}{\Delta+\gamma} \; 15.36(1.0 + 0.0062u_2) \; (e_z^o - e_z) \tag{4}$$

(Penman, 1948)

$$ET_{vB-B} = \frac{\Delta}{\Delta+\gamma}(R_n + G) + \frac{\gamma}{\Delta+\gamma} \; \frac{0.622\lambda\rho k^2}{P} \; \frac{u_z}{\ln(z/z_o)2} \; (e_z^o - e_z) \tag{5}$$

(van Bavel, 1966; Businger, 1956)

$$ET_{J-H} = C_T(T - T_x) \; R_s \tag{6}$$

(Jensen and Haise, 1963)

where

Δ = change in saturation vapor pressure with temperature
(millibars per degree Celsius);

$\gamma = \dfrac{c_p \; P}{0.622\lambda}$ = psychrometer constant (millibars per degree Celsius);

P = atmospheric pressure (millibars);

λ = latent heat of vaporization of water (calories per gram);

c_p = specific-heat capacity of air at constant pressure
(calories per gram per degree Celsius);

R_n = net radiation (langleys per day);

G = heat conducted to soil surface (langleys per day);

u_2 = wind speed at 2 m from ground (kilometers per day);

e_z^o = saturation vapor pressure at height z (millibar);

e_z = vapor pressure at height z (millibar);

31

Table 2.—*Evapotranspiration equations* —Continued

ρ = density of air (grams per cubic centimeter);

k = von Karman constant (=0.41);

u_z = wind speed at height z (centimeters per day);

z_0 = roughness parameter (centimeters);

C_T = $\dfrac{1}{C_1 + C_2 \; C_H}$ = temperature coefficient;

C_1 = 38 − (2 ℃ x elevation, in meters/305);

C_2 = 7.6 ℃;

C_H = $\dfrac{50 \text{ millibars}}{(e_2 - e_1)}$;

e_2 = saturation vapor pressure at mean maximum temperature for warmest month of year in area (millibars);

e_1 = saturation vapor pressure at the mean minimum temperature for warmest month of year in area (millibars);

T = air temperature (degrees Celsius);

T_x = −2.5 − 0.14 (e_2 − e_1) degrees Celsius/millibars − elevation, (in meters)/550; and
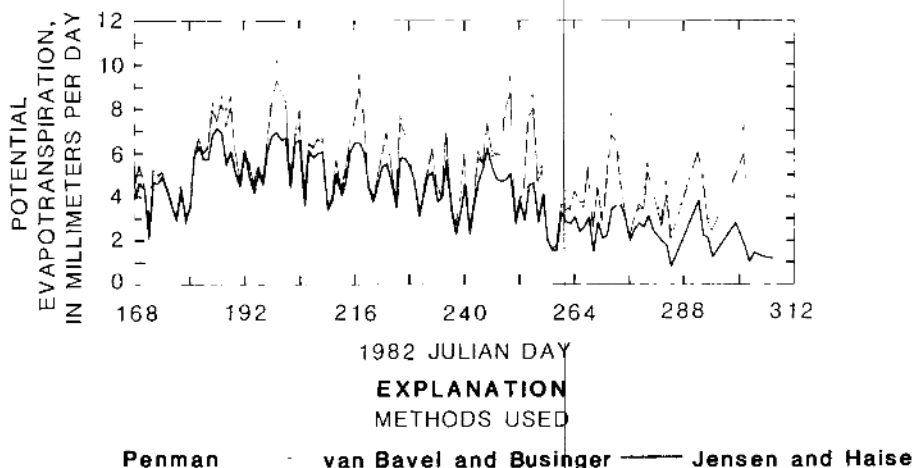
R_s = solar radiation (langleys per day).

Figure 20.—Estimates of 1982 potential evapotranspiration for Zenith site calculated by Penman, van Bavel and Businger, and Jensen and Haise methods.
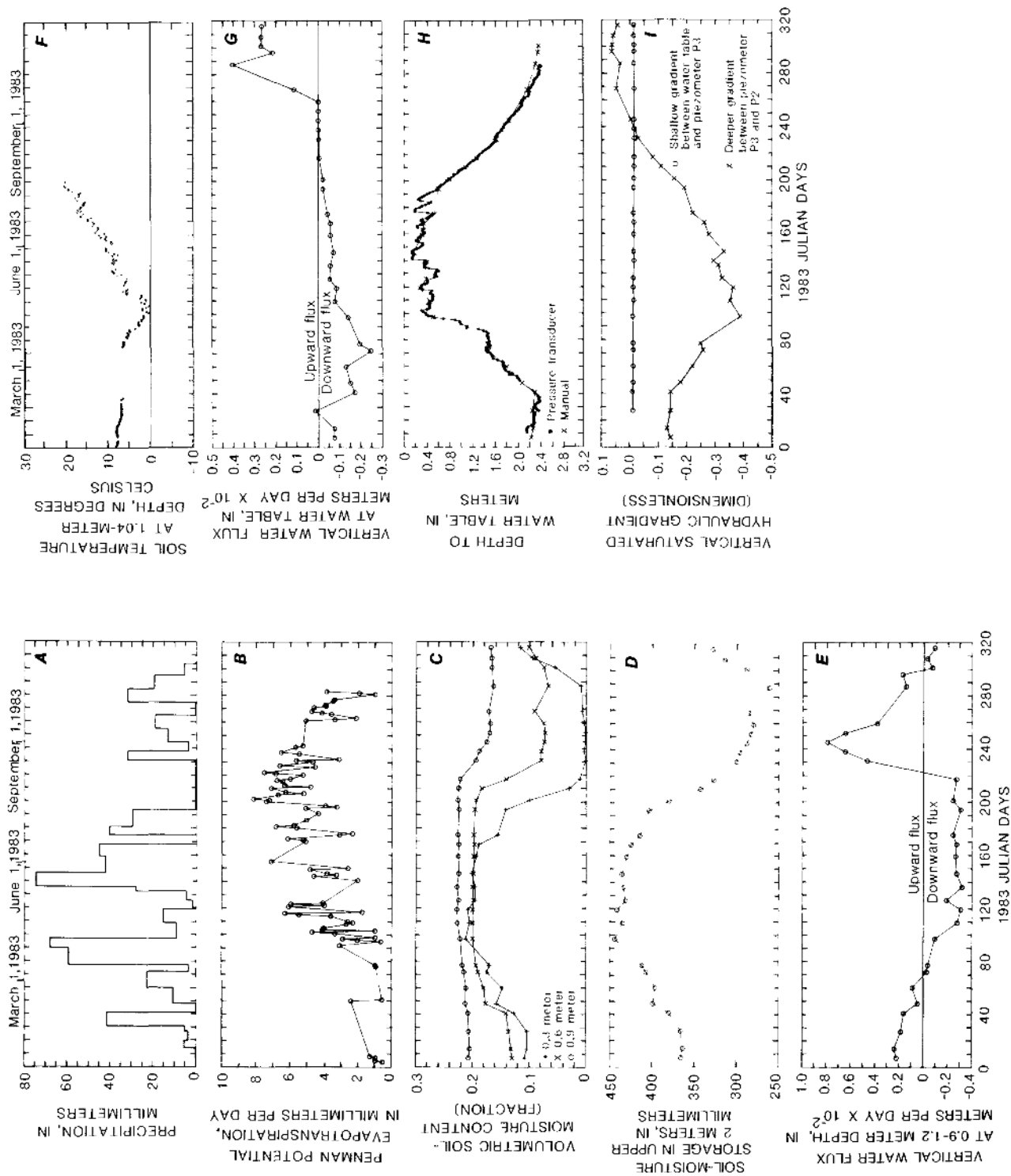
32

Figure 21.—Ground-water-recharge profile for Burrton site during 1983. (Time intervals lacking data symbols imply no data due to instrument malfunctions).

33

Calculated vertical water fluxes between 0.9 and 1.2 m (fig. 21e) and at the water table (fig. 21g) indicate downward movement. This is corroborated by the depression in soil temperature at 1.04 m (fig. 21f) and 1.34 m (not shown) due to the near-freezing temperature of infiltrating rain and snowmelt waters. As a result of flow to the water table, the water table rose nearly continuously during the effective-recharge period, as shown in figure 21h. The saturated hydraulic gradients near the water table (shallow gradient, fig. 21i) are nearly constant because any rise in water level in the water-table observation well was accompanied by a similar water-level rise in the shallowest piezometer (P3). This is in contrast with the hydraulic gradient between piezometers P3 and P2 (deeper gradient, fig. 21i), which shows more variable gradients. The deeper piezometers did not respond readily to water-level rises in the shallower water-table observation well and piezometer probably because of the increased clay content of the deeper sediments (fig. 4). This indicates that the shallower saturated flux is influenced by precipitation much more readily than the flux indicated by the deeper piezometers. The observed water-level rises, therefore, are due to precipitation and not due to lateral influxes.

To further support the last statement, a study of water-level fluctuations in nearby observation wells (shown by triangles in figure 3) and at the Burrton site indicates that wells in the area probably were not affected by irrigation withdrawals. Water levels in the nearby observation wells did not recover when irrigation pumpage stopped during September or October 1982 to January 1983, as is observed in aquifers affected by irrigation in south-central Kansas. Water levels in nearby observation wells declined from July 1982 to January 1983 and rose from January to July 1982 and from January to July 1983. The fact that water levels declined during the summer and fall 1982 and 1983 may be attributed to the absence of effective recharge during that period. For a recharge area, such as the Burrton area, a water-level decline is expected during periods without recharge. Note that no irrigation wells are located west of the Burrton site nor within 5 km north of the site. Irrigation wells are present south and southeast of the site, but irrigation pumpage there is fairly small, generally with water appropriations of less than 245 x 10^3 m^3/yr (64 Mgal/yr) per well. Therefore, the fact that relatively few irrigation wells exist in the vicinity of the site and that their pumpage is fairly small supports the contention that the water-level observations at the Burrton site may not have been affected by irrigation pumpage.

The resulting time distribution of effective recharge during February 10 (JD41) to May 26 (JD146), 1983, is shown in figure 21g of the recharge profile. The subsequent period of May 27 (JD147) to July 5 (JD186), 1983, although not contributing to higher water levels at the site, may still be considered as a recharge period in that the high water levels already achieved were maintained for the most part. After July 5 (JD186), 1983, a steady water-level decline followed (fig. 21h), which is coincident with little precipitation (fig. 21a) and rapid evapotranspiration rates (fig. 21b).

During February 10 (JD41) to May 26 (JD146), the water level rose by 2.1 m, as a result of 133.4 mm of effective recharge due to 296.9 mm of precipitation during that period. The effective-recharge estimate was calculated by summing all the products of point-flux measurements (fig. 21g) and the length of the associated recharge-time interval, which was chosen as the midpoint interval between point-flux measurements.

Snow depth on the ground during February 1-13 (JD32-44) progressively decreased from approximately 254 mm on February 2 (JD33) to 51 mm on February 13 (JD44). Since January 1983 was mostly dry (less than 10 mm of total precipitation from January 1 to 30), the total precipitation of 343 mm from January 31 (JD31) to May 26 (JD146), 1983, can be assumed safely to have contributed to the calculated 133 mm of effective recharge. Therefore, approximately 39 percent of the total precipitation during January 31 (JD31) to May 26 (JD146), 1983, was inferred to have contributed to the estimated effective recharge. Subsequently, during May 27 (JD147) to July 5 (JD186), 1983, an estimated 21 mm of additional direct recharge to the water table resulted from 158 mm of rainfall.

However, a significant part of this aquifer-recharge gain (approximately 68 percent, fig. 21g) from February 10 to July 5, 1983, was lost by an upward flux of water from September to mid-November. During the summer and fall of 1983, the evaporation front continued progressively deeper in the soil profile, as can be seen by (1) the drying of the soil profile during this period (fig. 21c and d), and (2) the large upward water flux in the 0.9-1.2 m soil layer (fig. 21e), which eventually continued downward to the water table (fig. 21g). Note the time lag and attenuation of the evaporation front as it spread from approximately the 1-m to the 2-m depth, as shown in figures 21e and 21g, respectively. Also note the reversal of the saturated hydraulic gradient (fig. 21i) between piezometers P2 (screened at approximately 17 m) and P3 (screened at approximately 12 m) from September to November 1983, indicating a transformation from a recharge to a discharge regime at the P3-P2 depth interval during the fall of 1983. However, such a reversal was not observed during the fall of 1982.

Zenith Site

The ground-water-recharge profile for the effective recharge period of April 7 (JD97) to June 29 (JD180), 1983, for the Zenith site is shown in figure 22. Because the data logger malfunctioned during most of the period from July 1983 onwards, precipitation values for the Hudson meteorological station, approximately 21 km northwest of the site (fig. 3), were used to supplement the Zenith site record after July 3 (JD184), 1983 (fig. 22a).

Two distinct periods of effective recharge can be recognized during this time interval. The first one caused a water-level rise of 0.17 m during April 7 (JD97) to 12 (JD102), 1983 (fig. 22h). This recharge event resulted from almost daily precipitation from March 19 (JD78) to April 12 (JD102), 1983, totaling 86 mm (fig. 22a). The water flux at the 1.2- to 1.5-m level, based on tensiometer readings, was downward, totaling less than 0.1 mm during this 6-day period. The flux at the water table during
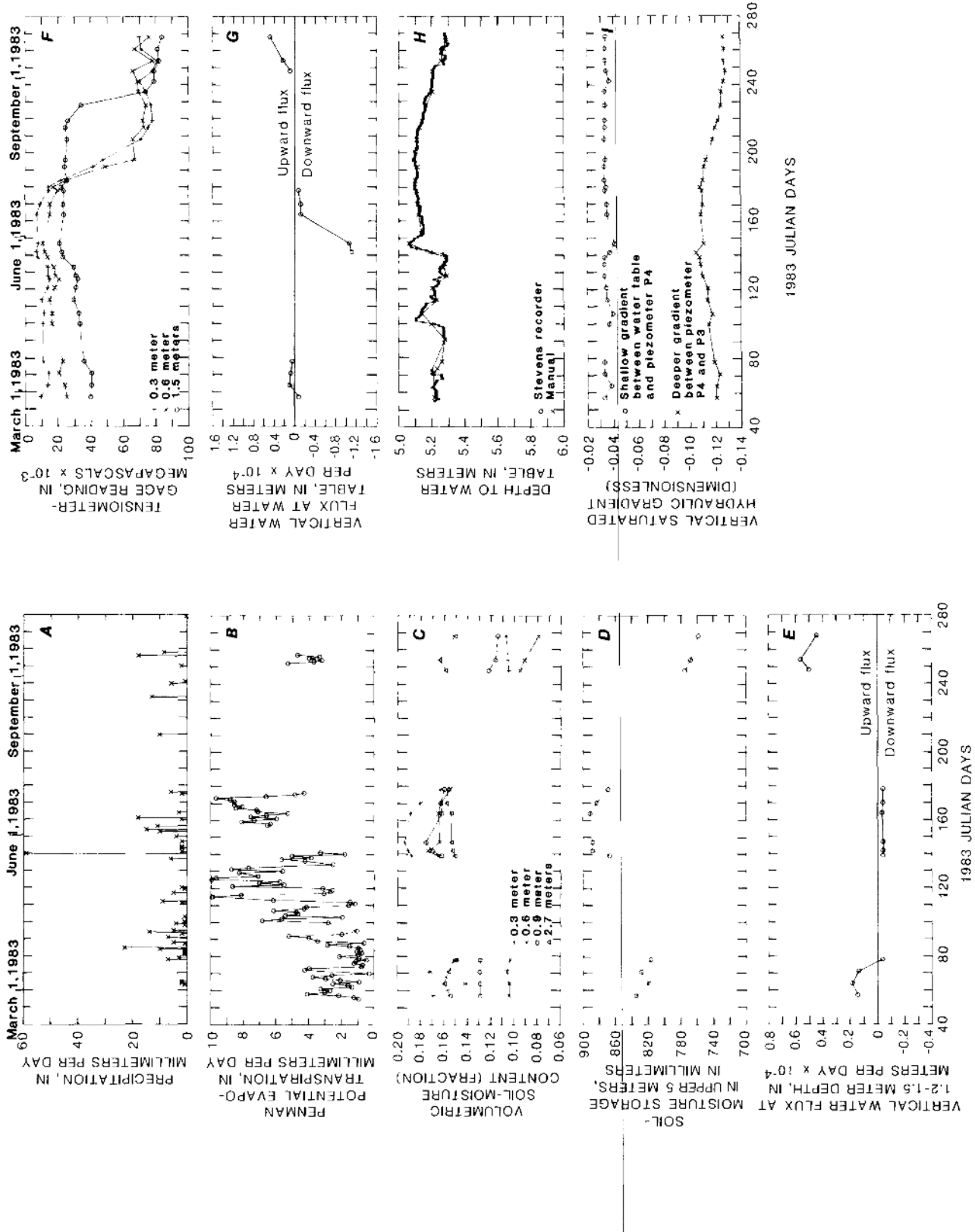
Figure 22.—Ground-water-recharge profile for Zenith site during 1983. (Time intervals lacking data symbols imply no data due to instrument malfunctions.)

this same period (fig. 22g) could not be estimated because of a malfunction of the neutron probe.

This first period of recharge was followed by a water-level decline, reaching its lowest point on May 19 (JD139), 1983 (fig. 22h). After April 12 (JD102), precipitation was not as frequent, reaching a total of 20 mm by April 30 (JD120), followed by no precipitation until May 17 (JD137), 1983 (fig. 22a).

A second period of recharge caused a water-level rise of 0.22 m from May 19 (JD139) to May 27 (JD147) and resulted from 72 mm of precipitation during May 17-27 (JD137-147). The flux at the water table during this second recharge period totaled approximately 0.9 mm. This rise in the water level was followed by a small decline (fig. 23h) until June 4 (JD155), 1983, after which a gradual, small rise (0.05 m) in the water levels was observed until about June 29 (JD180), 1983, probably due to 63 mm of precipitation from May 28 (JD148) to June 13 (JD164), 1983; only 8 mm of rain occurred after then until June 29 (JD180).

Although the two relatively sharp water-level rises observed at the Zenith site (fig. 22h) most probably were caused by local recharge, the gradual water-level rise from June 4 to 29 (JD155-180), 1983, probably was due to a combination of local recharge and regional flow from the west (refer to figure 8) because a gradual water-level rise during this period was observed in the deeper piezometers (P2, P3, P4) as well, without any noticeable time lag in the piezometer responses. Rainfall amounts for June 1983, were lowest at the site (67 mm), increasing westward with 85 mm at Pratt, approximately 58 km west-southwest, and 168 mm at Larned, approximately 60 km west-northwest from the Zenith site.

Water levels started declining slowly after June 29 (JD180), 1983 (fig. 22h). This water-level decline is coincident with the drying soil profile (figs. 22c, d, and f) and upward moisture flow (figs. 22e and g). The flux at the water table during May 28 (JD148) to June 29 (JD180) was approximately 1.2 mm (fig. 22g). Thus, a total of 2.1 mm of recharge occurred during May 19 (JD139) to June 29 (JD180) as a result of 153.9 mm of precipitation since May 17 (JD137). Thus, only 1.4 percent of this precipitation resulted in recharge. As was observed also at the Burrton site, a part (although smaller than at Burrton) of this aquifer-recharge and soil-moisture-storage gain was lost by evaporative fluxes during August through October 1983, as can be seen from figures 22c through h.

The hydraulic-head gradient near the water table (fig. 22i) was fairly constant during the period of record, with two peaks coinciding approximately with the two reported recharge periods. The hydraulic gradient between piezometers P4 at the 23-m depth and P3 at the 31-m depth increased during summer and fall due to the steeper water-level decline in the deeper piezometer P3 compared to that of P4, which follows the water-level decline more closely. The thick clay layer in the vertical interval between piezometers P4 and P3 (fig. 4) seems the likely reason for this observation. The nearby observation wells (fig. 3) at the Zenith site show a consistent water-level rise for January to June 1983, followed by a water-level decline.

Comparison of Recharge Estimates and Possible Sources of Error

The large difference between the estimated recharge at the Burrton site (154 mm) and the estimated recharge at the Zenith site (2.1 mm) was expected as a result of 159 mm more precipitation and less evapotranspiration at Burrton. However, to check this result, the hydraulic conductivity corresponding to the average moisture content at the 0.9- to 1.2-m depth interval at the Zenith site (see section on "Hydraulic-Conductivity Function") and thus the reference-flux values at the same depth interval were increased by one order of magnitude. Equation (2) then was employed to calculate the fluxes at the water table during the May 19 to June 29 (JD139–180), 1983, recharge period. The resulting recharge amount of 3.0 mm during this time amounted to approximately 1.9 percent of the total precipitation (153.9 mm) during the same time interval, compared to approximately 1.4 percent calculated previously, a number which still is very small compared to the recharge estimate at the Burrton site.

Table 3 summarizes the significant differences between recharge-related variables for the Burrton and Zenith sites during the major recharge period of March 1 (JD60) to June 30 (JD81), 1983. Precipitation was greater for the Burrton site--414 mm (fig. 21a) than for the Zenith site--255 mm (fig. 22a), and the estimated average daily potential evapotranspiration during the same time period was greater for the Zenith site (4.4 mm/d, fig. 22b) than for the Burrton site (3.7 mm/d, fig. 21b). Finally, note that the approximate average soil-moisture storage in the upper 1.2 m was greater (265 mm) for the Burrton site (fig. 21h) than for the Zenith site (193 mm, fig. 22h). As a result, the average volumetric moisture content for the top 1.2 m of soil at the Burrton site was approximately 21.7 percent as compared to 15.8 percent at the Zenith site. Precipitation at the Zenith site during this period was approximately 62 percent of the precipitation at the Burrton site; however, the estimated recharge for the Zenith site amounted to less than 1.5 percent of that estimated for the Burrton site.

Table 3.--*Comparison of recharge-related variables for the Burrton and Zenith sites*

Recharge period March 1 (JD60) - June 30 (JD181), 1983	Burrton site	Zenith site
Precipitation (millimeters)	414	255
Potential evapotranspiration (millimeters per day)	3.7	4.4
Depth-to-water range (meters)	1.75-0.15	5.30-5.05
Soil-moisture storage in upper 1.2 meters (millimeters)	265	193
Average volumetric soil-water content ($\theta_{ave.}$) in upper 1.2 meters (dimensionless)	.217	.158
Unsaturated hydraulic conductivity at $\theta_{ave.}$ (meters per day)	6.5×10^{-4}	3×10^{-6}

The reliability of ground-water-recharge estimates depends on the accuracy of estimated soil-water characteristic functions and unsaturated hydraulic-conductivity functions for the vadose zone. Soil-water measurements with a neutron probe can be precise to less than 1 percent with correct use. The main sources of error in neutron-probe usage are inaccurate calibration, soil damage from access-tube installation, damage to surface soil and vegetation, water traveling along the access tube or seeping into the access tube, relocation error, random-count error, large temperature differential between the probe that is lowered into the access tube and the surface unit containing counting and display circuit batteries, and inherent soil variability. Sources of error in tensiometry are entrapped air bubbles and leaks, variations with temperature, loss of porous-cup contact with the soil, water traveling along the shaft, and errors in reading the dial.

Hysteresis effects preclude accurate determination of onsite soil-water characteristic curves for the unsaturated zone. The error probably is compounded further by the use of mean characteristic curves to translate neutron-moisture readings to hydraulic-head values. Determination of unsaturated hydraulic-conductivity functions, as was mentioned earlier, is difficult and time consuming both onsite and in the laboratory, with the difficulty and uncertainty increasing with increasing soil dryness. These problems are compounded by the inherent large degree of spatial variability, which precludes the application of the hydraulic-conductivity function for a given soil to any other location.

Because neither replicate hydraulic-conductivity or desaturation experiments were conducted on the same samples nor were sufficient samples from the same depth interval collected and analyzed for these physical properties, statistical-error analysis could not be performed. Furthermore, because no onsite hydraulic-conductivity experiments for comparison with laboratory experiments were conducted, assessment of the hydraulic-conductivity error component was not attempted.

The key to increasing the reliability of ground-water-recharge estimates lies with the determinations of the hydraulic-conductivity and soil-water characteristic functions. Because of the sources of error mentioned earlier, recharge estimates, such as the ones presented here, should only be considered as approximate.

RELATION OF METEOROLOGICAL AND SOIL-WATER CONDITIONS

TO RECHARGE EVENTS

A certain amount of moisture buildup in that part of the soil zone that is influenced by evapotranspiration is needed for effective ground-water recharge to occur. In a comprehensive study on the mechanisms of ground-water recharge, Freeze (1969) concluded that of all the factors controlling ground-water recharge, the antecedent soil-moisture regime probably is the most important. The driest and wettest soil-moisture profiles for both recharge sites, as well as the moisture profiles just

39

prior to effective recharge, are presented in figure 23. The driest pro-
files, which occurred after a long period of little or no precipitation
and significant evapotranspiration, may be considered as approximating
residual-moisture profiles; that is, minimum-moisture profiles after the
effects of gravity drainage and evapotranspiration become negligible. The
moisture profiles observed just before effective recharge was initiated
may be reasonably assumed to have reached their water-holding capacity.

EXPLANATION

SOIL-MOISTURE PROFILES

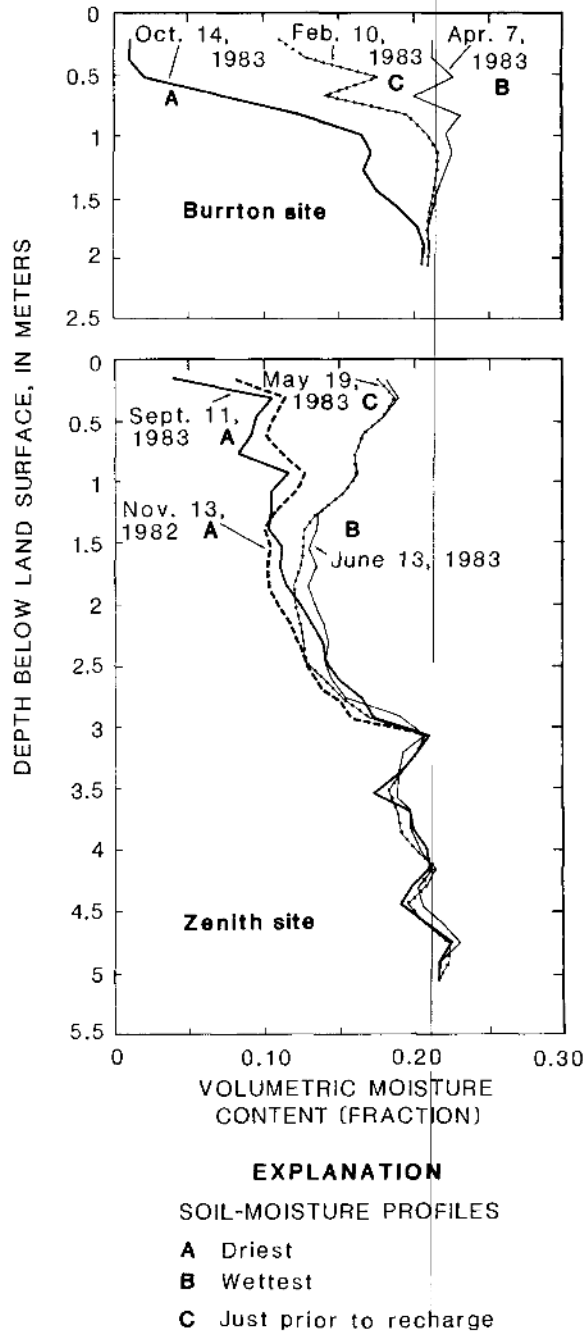A   Driest
B   Wettest
C   Just prior to recharge

Figure 23.--Driest and wettest observed soil-moisture profiles during
1982-83 for Burrton and Zenith sites.

Late November to mid-February represents the period during which the already-dry moisture profiles effectively built up moisture at the Burrton site. The January and early February 1983, moisture profiles can be reasonably assumed to closely approximate their water-holding capacity, which in water-depth-equivalent terms for the top 2 m of the profile totaled about 369 mm. Since the driest observed profile of October 14 (JD287), 1983 (fig. 24), can be assumed to represent the residual-moisture profile totaling 261 mm, the moisture buildup required before initiation of effective recharge for Burrton is approximately 108 mm.

For the Zenith site with the longer unsaturated soil profile (approximately 5.03 m), the overall choice of the driest or wettest profile is made by calculating the equivalent depth of water stored in the entire profile. This choice is made because individual sections of the soil profile may be wetter or drier than the selected one at different times. The driest profiles for both 1982 and 1983 for the Zenith site are shown in figure 23. The November 1982, profile represents the driest one for the 1.2- to 3.0-m depth interval, while the September 1983, profile represents the driest one for the 0- to 1.2-m depth interval. The moisture mounding at approximately the 2.4-m level (fig. 23) above the sandy clay loam and clay loam layers (fig. 6), even during the 1983 driest overall profile, indicates the partially confining nature of that layer.

Mid-November to March represents the period of effective soil-moisture buildup for the Zenith site. Note that during this time period, evapotranspiration-moisture losses are at their minimum (fig. 22b). The May 1983 moisture profiles can be assumed to closely approximate their water-holding capacity, which in depth-water-equivalent terms totals about 881 mm. Since the driest overall moisture profile of September 11 (JD754), 1983 (fig. 23), can be assumed to approximate the residual-moisture profile totaling approximately 767 mm, the moisture buildup required for initiation of effective recharge for Zenith is approximately 114 mm. The generally sandier nature of the Zenith soil profile (fig. 6) down to the 3-m depth level and the nearly constant moisture distribution beyond that depth during the study period may help explain the relatively small moisture buildup required for the Zenith profile before effective recharge can take place.

During most of this study, the moisture profiles in general were nearly constant below approximately 0.9 m for Burrton and 2.7 m for Zenith, with both depth levels corresponding to a transition from sandy loam to sandy clay loam. In general, evapotranspiration losses below these depths were relatively minor. However, during severe dryness, these evapotranspiration-depth levels could move downward as was observed, particularly at the Burrton site, during the dry period of July through October 1983 (fig. 21).

The most effective way to build up soil moisture in the profile is through frequent rainfall over a period of time with relatively small evapotranspiration losses, as occurs during winter and early spring. In addition to rainfall, snowmelt is effective in building up soil moisture. For example, the first recharge period observed at the Burrton site during mid-February 1983, was due predominantly to the melting of accumulated

snow on the ground at the site. During site visitation, a snow depth of approximately 178 mm was observed on February 10, 1983 (JD41), and no snow was observed on February 17, 1984 (JD48). During this period no precipitation fell at the site or on the surrounding area. Also, freezing temperatures were recorded at the site and in the general area up to February 10 (JD41), after which snowmelt started. The observed soil-moisture and water-table rises during this and subsequent periods, together with the unusually depressed soil temperatures observed after snowmelt (fig. 21f), support these observations.

Significant summer rainfall or thunderstorms at both recharge sites did not contribute to recharge during the study period. The effect of summer and fall precipitation for July 1 (JD182) to October 15 (JD259), 1982, at the Zenith recharge site, for example, is analyzed in figure 24. Two major storms occurred during this period (fig. 24a), one on August 16 (JD228), totaling 15.0 mm, and one on September 16 (JD259), totaling 28.2 mm. These storms clearly penetrated only the top 0.3 m of the soil profile at the Zenith site and did not affect the 0.6-m depth level as can be seen clearly by observing the gypsum-block response at the 0.3- and 0.6-m depth (fig. 24d and e).

At both recharge sites the excess water during storms was observed to accumulate in numerous shallow depressions, thus forming ephemeral ponds that evaporated quickly under the prevailing rapid potential-evapotranspiration environment (fig. 24b). The tensiometer-transducer data for 0.15-m depth averaged over a daily period together with time-instant dial-gage readings also are shown (fig. 24c). Soil-moisture depletion during the hot, dry periods of summer and the temporary moisture buildup during storms also are shown in figure 24f.

Longer duration high- or low-intensity rainfalls may contribute to effective ground-water recharge. For example, the high-frequency and high-intensity rainfall combination at the Burrton site during March 26 (JD85) to April 5 (JD95), and May 11 (JD131) to May 29 (JD149), 1983, maintained nearly a constant rate of ground-water recharge. The almost daily rainfall at the Zenith site during March 19 (JD78) to April 12 (JD102), 1983, contributed to effective recharge during April 7-12. Note that the second observed period of effective recharge at Zenith during May 19-28 (JD139-148), 1983, was not preceded by a high-frequency or high-intensity rainfall but was caused almost solely by a practically continuous 24-hour rainfall totaling 58.9 mm on May 20 (JD140). The resulting water-table rise was maintained by frequent high-intensity rainfall immediately following from May 30 (JD150) to June 13 (JD164).

If one considers the record of Hutchinson 10SW meteorological station (fig. 3), which is approximately equidistant between the two sites, as representative of precipitation at the study sites, then that station's 1982 total precipitation of approximately 676 mm is less than the 1960-83 average of 729.0 mm, while the 1983 total precipitation of 785 mm is greater than average. The major moisture buildup during December 1982 through February 1983, in the soil at both sites as implied by the records at nearby meteorological stations was characterized by greater-than-average precipitation (113-mm average at the Hutchinson 10SW station compared to the 71.5-mm long-term average) and contributed to the observed 1983 recharge at both sites.
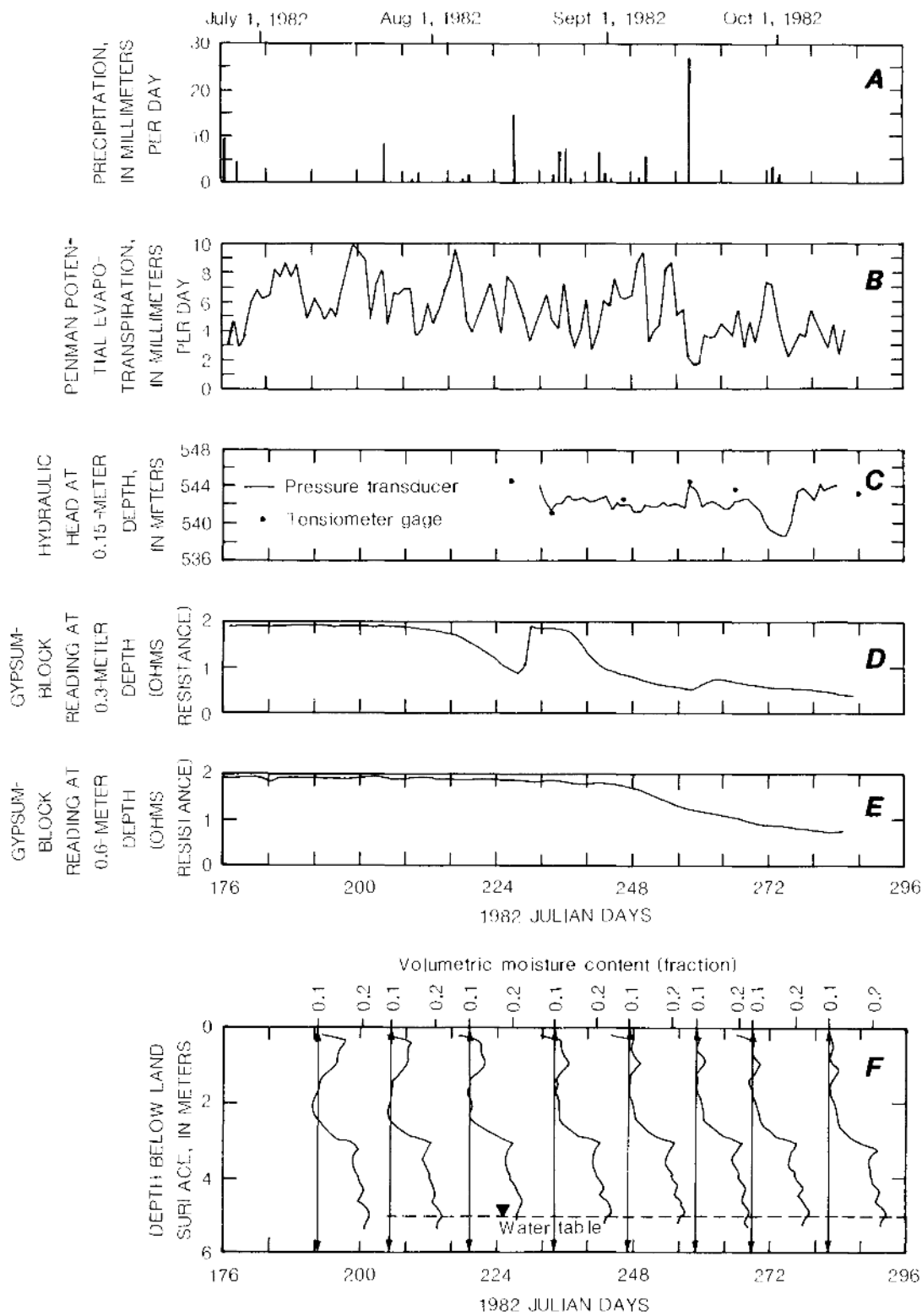
42

Figure 24.--Effect of 1982 summer and fall precipitation on ground-water recharge at Zenith site.

CONCLUSIONS

The goal of this study, which was the determination of the amount and time distribution of ground-water recharge from precipitation at two specific sites in south-central Kansas, has been achieved. Recharge occurred only during late winter and spring; no recharge occurred in late summer and fall, and the estimated recharge amounts were significantly different for the two recharge sites, ranging from approximately 154 mm at Burrton to less than 2.5 mm at Zenith. However, a significant part of this predominantly springtime recharge was lost by evapotranspiration during late summer and fall, especially at the Burrton site (68 percent) because of its shallow water table.

Both sites are located in sand-dune areas in natural ground-water-recharge areas (as opposed to discharge areas) with similar sandy soils characterized by underlying, relatively thin clayey layers, typical of south-central Kansas. The reader is cautioned against generalizing the estimated recharge rates found in this study over large areas because such results represent only two relatively short-term point measurements in the extensive sand-dune areas of south-central Kansas. Therefore, the recharge estimates presented here should be regarded only as approximate.

The main cause of the large differential in recharge estimates observed at the two sites was the greater precipitation and lesser potential evapo-transpiration at the Burrton site. Another cause was the greater thickness of the unsaturated zone and the smaller average moisture content in that zone at Zenith. This smaller moisture content resulted in a corresponding decrease in the average unsaturated hydraulic conductivity compared to the average unsaturated hydraulic conductivity at the Burrton site. Soil layer-ing in the unsaturated zone, such as the progression from sandy loam to sandy clay loam to clay loam at the Zenith site (fig. 6) played an important part in facilitating or restricting downward water movement.

For studies such as this one, where hysteresis effects have not been analyzed in detail, calculation of water fluxes in the unsaturated zone based on site-derived "average" soil-water characteristic curves may be more advantageous than using tensiometer data for flux calculations. For cases of predominantly vertical unsaturated water fluxes and a measured reference water flux in the upper soil profile, simple integration of the one-dimensional water-balance equation was found to be an effective way of translating an upper-layer flux to a deeper-water flux at the water table. This procedure, however, requires a neutron-probe access tube penetrating below the water table and its expected range of fluctuation. The combination of soil-water characteristic curves and saturated hydraulic conductivity provided a relatively simple way of predicting the unsaturated hydraulic-conductivity functions used in this study, given that the onsite water content at the soil depths at which flux calculations were carried out was not near the extreme dry-moisture ranges and that the soils were not too clayey.

Despite the numerous instrumentation problems discussed, most of the sensors performed satisfactorily. All atmospheric sensors connected to the CR-21 data logger operated within expectations, as did the neutron

44

probe. The water-level pressure transducer performed well after wiring problems were corrected, as did the Stevens graphical recorders. Nevertheless, the tensiometer system was not very reliable over long periods of time, and periodic recalibrations of the system were required. However, the dual system for each depth worked to provide long-term records. The pressure transducer used with the tensiometers needs to be made less sensitive to environmental conditions. Several suggestions for improving instrument performance and minimizing data losses resulted from this study.

The built-in programmable memory of modern data loggers was valuable for data manipulation and interpretation. Such data loggers can provide on- and offsite data-processing capabilities, such as calculating maximum, minimum, and mean values over specified time intervals, plotting histograms, and obtaining standard deviations and times of extreme events. They can interface with cassette tapes, telephone lines, radio transmitters, and even satellites. These data loggers are portable, have small power requirements, and are quite versatile.

Theoretical advances in hydrosciences have exceeded advances in experimental research. Coupled mass and energy flow of multiphase fluids in unsaturated-saturated porous media can be numerically simulated, but appreciable difficulties are encountered during onsite measurement of the required characteristics to implement these models. For example, considerable difficulties are recognized in obtaining onsite and laboratory measurements of unsaturated hydraulic conductivity over a wide range of moisture contents; or in obtaining continuous long-term tensiometer records, or just simple tensiometer records at depths greater than 2 m. Perhaps through specific research in perfecting experimental measurements, onsite measurements will be improved and simplified.

REFERENCES

American Society for Testing Materials, 1979, 1979 annual book of American Society for Testing Materials standards: American Society for Testing Materials, part 19, 632 p.

Black, C.A., ed., 1965, Methods of soil analysis: American Society of Agronomy, Agronomy No. 9, part 1, 770 p.

Brooks, R.H., and Corey, A.T., 1964, Hydraulic properties of porous media: Ft. Collins, Colorado State University, Hydrology Paper No. 3, 27 p.

Businger, J.A., 1956, Some remarks on Penman's equations for the evapotranspiration: Netherlands Journal of Agricultural Science, v. 4, p. 77-80.

Childs, E.C., and Collis-George, N., 1950, The permeability of porous materials: Proceedings of Royal Society, part A, p. 201, 392-405.

Danielson, R.E., 1982, Soil physics laboratory manual: Ft. Collins, Colorado State University, Agronomy Department, 70 p.

Duke, H.R., 1972, Capillary properties of soils--Influence upon specific yield: Transactions of American Society of Agricultural Engineering, v. 15, no. 4, p. 688-691.

Farnsworth, R.K., and Thompson, E.S., 1982, Mean monthly, seasonal, and annual pan evaporation for the United States: National Oceanic and Atmospheric Administration Technical Report 34, U.S. Department of Commerce, National Weather Service, 82 p.

Freeze, R.A., 1969, The mechanism of natural ground-water recharge and discharge--1. One-dimensional, vertical, unsteady, unsaturated flow above a recharging or discharging ground-water flow system: Water Resources Research, v. 5, p. 153-171.

Freeze, R.A., and Banner, James, 1970, The mechanism of natural ground-water recharge and discharge--2. Laboratory column experiments and field measurements: Water Resources Research, v. 6, p. 138-155.

Gardner, W.H., 1965, Water content, in Methods of soil analysis, C.A. Black, ed.: American Society of Agronomy, Agronomy No. 9, part 1, p. 82-127.

Howard, K.W.F., and Lloyd, J.W., 1979, The sensitivity of parameters in the Penman evaporation equations and direct recharge balance: Journal of Hydrology, v. 41, p. 329-344.

Jackson, R.D., Reginato, R.J., and van Bavel, C.H.M., 1965, Comparison of measured and calculated hydraulic conductivities of unsaturated soil: Water Resources Research, v. 1, p. 375-380.

Jensen, M.E., 1966, Empirical methods of estimating or predicting evapotranspiration using radiation: Proceedings of the Conference on Evapotranspiration, American Society of Agricultural Engineers, Chicago, Ill., Dec. 1966, p. 57-61.

Jensen, M.E., ed., 1973, Consumptive use of water and irrigation water requirements: American Society of Civil Engineers, 215 p.

Jensen, M.E., and Haise, H.R., 1963, Estimating evapotranspiration from solar radiation: American Society of Civil Engineers, Journal of Irrigation and Drainage Division, v. 89, p. 15-41.

Jensen, M.E., Robb, D.C.N., and Franzoy, C.E., 1970, Scheduling irrigations using climate-crop-soil data: American Society of Civil Engineers, Journal of Irrigation and Drainage Division, v. 96, p. 25-38.

Kansas Geological Survey, 1964, Geologic map of Kansas: Kansas Geological Survey Map M-1, scale 1:500,000, 1 sheet.

Kimball, B.A., and Jackson, R.D., 1975, Soil heat flux determinations-- A null alignment method: Agricultural Meteorology, v. 15, p. 1-9.

Kunze, R.J., Uehara, G., and Graham, K., 1968, Factors important in the calculation of hydraulic conductivity: Proceedings of American Soil Science Society, v. 32, p. 767-765.

Lohman, S.W., and Frye, J.C., 1940, Geology and ground-water resources of the Equus beds area in south-central Kansas: Economic Geology, v. 35, no. 7, p. 839-866.

Marshall, T.J., 1958, A relation between permeability and size distribution of pores: Journal of Soil Science, v. 9, p. 1-8.

Millington, R.J., and Quirk, J.P., 1959, Permeability of porous media: Nature, v. 183, p. 387-388.

_____1961, Permeability of porous solids: Transactions of Faraday Society, v. 57, p. 1220-1207.

National Semiconductor Corporation, 1977, Pressure transducer handbook: Santa Clara, California, National Semiconductor Corp., 130 p.

_____1981, Pressure transducer data booklet: Santa Clara, California, National Semiconductor Corp., 68 p.

Nielsen, D.R., Biggar, J.W., and Erh, K.T., 1973, Spatial variability of field measured soil-water properties: Hilgardia, v. 42, no. 7, p. 215-259.

Penman, H.L., 1948, Natural evaporation from open water, bare soil and grass: Proceedings of Royal Society, series A, v. 193, p. 120-146.

_____1963, Vegetation and hydrology: Commonwealth Bureau of Soils, Technical Communication No. 53, 125 p.

Rockers, J.J., Ratcliff, Ivan, Dowd, L.W., and Bouse, E.F., 1966, Soil survey of Reno County Kansas: U.S. Department of Agriculture, Soil Conservation Service, 72 p.

Rose, C.W., Stern, W.R., and Drummond, J.E., 1965, Determination of hydraulic conductivity as a function of depth and water content for soil in situ: Australian Journal of Soil Research, v. 3, p. 1-9.

Shaukat, Nadeem, and Sophocleous, M. A., 1983, Evaluation of predictive methods of hydraulic conductivity based on porous media properties: Kansas Geological Survey Open-File Report 83-31, 197 p.

Sophocleous, M.A., 1979, Analysis of water and heat flow in unsaturated-saturated porous media: Water Resources Research, v. 15, no. 5, p. 1195-1206.

_____1983, Groundwater observation network design for the Kansas Groundwater Management Districts, USA: Journal of Hydrology, v. 61, p. 371-389.

_____1985, The role of the unsaturated zone in ground-water-recharge estimations--A numerical study: Ground Water, v. 22, no. 1, p. 52-58.

van Bavel, C.H.M., 1966, Potential evaporation--The combination concept and its experimental verification: Water Resources Research, v. 3, no. 3, p. 455-467.

van Bavel, C.H.M., Stirk, G.B., and Brust, K.J., 1968, Hydraulic properties of a clay loam soil and the field measurement of water uptake by roots--Interpretation of water content and pressure profiles: Proceedings of American Society of Soil Science, v. 32, p. 310-317.

Warrick, A.W., and Nielsen, D.R., 1980, Spatial variability of soil physical properties in the field, in Application of soil physics, by D. Hillel: New York, Academic Press, p. 319-344.